Understanding Gravitational Waves through Numerical Simulations

by

Lorenzo Speri

THESIS

for the degree of

BACHELOR OF SCIENCE

Physics
University of Trento

May 2018

Contents

Abstract

A really interesting and fascinating abstract

1 Introduction

Albert Einstein developed the General Theory of Relativity between and 1907 and 1917, creating a new tool to observe the universe. The General Theory of Relativity has changed the way we describe and study the gravitational phenomena. In particular, the new theory of gravitation was not only able to solve unexplained observations, as for instance, anomalies in the newtonian description of planets' orbits as Mercury, but it also predictied new phenomena such as gravitational time dilation, gravitational lensing and gravitational waves. The first indirect detection of general relativity was made by Hulse and Taylor. One of the most important test of the General Theory of Relativity was the discovery of the gravitational waves (GW) at LIGO.

NOTATION: we use a system of geometrized units $G = c = 1$.
Greek letters for summing over all the indeces from 0 up to 3. Latin letters summing only on the spatial indeces 1 2 and 3. Sometimes we use boldface to denote the spatial vectors $\mathbf{x} = (x, y, z)$ and we rewrtie the four-vectors as

$$x^\sigma = (x^0, x^1, x^2, x^3) = (t, \mathbf{x}) = (t, x, y, z)$$

2 From the Einstein's field equation to gravitational wave solutions

Albert Einstein developed the General Theory of Relativity between and 1907 and 1917, creating a new tool to observe the universe. The General Theory of Relativity has changed the way we describe and study the gravitational phenomena. In particular, the new theory of gravitation was not only able to solve unexplained observations, as for instance, anomalies in the newtonian description of planets' orbits as Mercury, but it also predictied new phenomena such as gravitational time dilation, gravitational lensing and gravitational waves. One of the most important test of the General Theory of Relativity was the discovery of the gravitational waves (GW).

2.1 Linearized Einstein's field equation

The Einstein's field equation represents how the geometry of space-time is related to the presence of masses and energy:

$$G_{\mu\nu} \equiv R_{\mu\nu} - \frac{1}{2}\, g_{\mu\nu}\, R = \frac{8\,\pi\, G}{c^4}\, T_{\mu\nu} \tag{1}$$

On the right hand side we have the energy-momentum tensor $T_{\mu\nu}$, which is interpreted as the flux of four momentum p^μ accross a surface of constant x^ν, and $G = 6.67408 \times 10^{-11}\,\mathrm{N\ m^2\ kg^{-2}}$ and $c = 299\,792\,458\,\mathrm{m/s}$ that are respectively the Newton constant of gravitation and the speed of light. On the left hand side the Einstein tensor $G_{\mu\nu}$ includes a measure of the curvature of spacetime through the Ricci tensor $R_{\mu\nu}$, the Ricci scalar $R = R_{\mu\nu} g^{\mu\nu}$ and the metric $g_{\mu\nu}$.
In order to solve the Einstein's equation we will make assumptions on the metric tensor $g_{\mu\nu}$ and we will derive the Einstein tensor $G_{\mu\nu}$ going through the following steps:

(a) Calculate the Christoffel symbol

$$\Gamma^{\alpha}{}_{\beta\gamma} = \frac{1}{2} g^{\alpha\rho} \left(\partial_\beta g_{\gamma\rho} + \partial_\gamma g_{\rho\beta} - \partial_\rho g_{\beta\gamma}\right) \tag{2}$$

where ∂_μ means the partial derivative $\partial/\partial x^\mu$.

(b) Calculate the Riemann curvature tensor

$$R^{\alpha}{}_{\beta\gamma\sigma} = \Gamma^{\alpha}{}_{\gamma\lambda}\,\Gamma^{\lambda}{}_{\sigma\beta} - \Gamma^{\alpha}{}_{\sigma\lambda}\,\Gamma^{\lambda}{}_{\gamma\beta} + \partial_\gamma \Gamma^{\alpha}{}_{\sigma\beta} - \partial_\sigma \Gamma^{\alpha}{}_{\gamma\beta} \tag{3}$$

(c) Obtain the Ricci tensor and the Ricci scalar from the Riemann curvature tenor

$$R_{\mu\nu} = R^{\alpha}{}_{\mu\alpha\nu} \qquad\qquad R = \eta^{\mu\nu} R_{\mu\nu} = R^{\mu}{}_{\mu} \tag{4}$$

$G_{\mu\nu}$ and $T_{\mu\nu}$ are symmetric tensors because $g_{\mu\nu}$ is symmetric as well. So the Einstein's field equation is a set of non-linear second-order partial differential equations with 10 linearly independent variables.
We show that the equation(1) leads to gravitational wave solutions if we consider a weak gravitational field, where the spacetime is nearly flat. Therefore, we assume the metric tensor $g_{\mu\nu}$ to be equal to the Minkwoski metric $\eta = \mathrm{diag}(-1, +1, +1, +1)$ plus a small perturbation $h_{\mu\nu}$:

$$g_{\mu\nu} = \eta_{\mu\nu} + h_{\mu\nu} \tag{5}$$

where perturbation is symmetric and $|h_{\mu\nu}| \ll 1$ for all μ and ν.
The metric $g_{\mu\nu}$ is also used to lower and raise indeces, however, in linearized theory we consider only the first order approximation in $h_{\mu\nu}$. So, it is possible to raise and lower indeces using the Minkoswkian metric $\eta_{\mu\nu}$.
Taking into account the mentioned approximations we follow the described procedure to calculate the so-called linearized Einstein's field equation. The Christoffel symbol is obtained keeping up to the first order in the perturbation $h_{\mu\nu}$

$$\Gamma^{\alpha}{}_{\beta\gamma} = \frac{1}{2}\eta^{\alpha\rho}(\partial_\beta h_{\gamma\rho} + \partial_\gamma h_{\rho\beta} - \partial_\rho h_{\beta\gamma})$$

The Riemann curvature tensor is

$$\begin{aligned} R^{\mu}{}_{\beta\gamma\nu} &= \partial_\gamma \Gamma^{\mu}{}_{\nu\beta} - \partial_\nu \Gamma^{\mu}{}_{\gamma\beta} \\ &= \frac{1}{2}[\eta^{\mu\rho}(\partial_\gamma\partial_\nu h_{\beta\rho} + \partial_\gamma\partial_\beta h_{\nu\rho} - \partial_\gamma\partial_\rho h_{\beta\nu}) - \eta^{\mu\sigma}(\partial_\nu\partial_\beta h_{\gamma\sigma} + \partial_\nu\partial_\gamma h_{\beta\sigma} - \partial_\nu\partial_\sigma h_{\beta\gamma})] \\ &= \frac{1}{2}\big(\partial_\gamma\partial_\beta h^{\mu}{}_{\nu} - \partial_\gamma\partial^{\mu} h_{\beta\nu} - \partial_\nu\partial_\beta h^{\mu}{}_{\gamma} + \partial_\nu\partial^{\mu} h_{\beta\gamma}\big) \end{aligned} \tag{6}$$

where we neglected the first two terms in eq(3) because they are second order terms. Contracting the first and the third indeces we get the Ricci tensor

$$\begin{aligned} R_{\beta\nu} &= \frac{1}{2}\big(\partial_\mu\partial_\beta h^{\mu}{}_{\nu} - \partial_\mu\partial^{\mu} h_{\beta\nu} - \partial_\nu\partial_\beta h^{\mu}{}_{\mu} + \partial_\nu\partial^{\mu} h_{\beta\mu}\big) \\ &= \frac{1}{2}(\partial_\mu\partial_\beta h^{\mu}{}_{\nu} - \Box h_{\beta\nu} - \partial_\nu\partial_\beta h + \partial_\nu\partial^{\mu} h_{\beta\mu}) \end{aligned}$$

where the trace of the perturbation is defined as $h = \eta^{\mu\nu}h_{\mu\nu} = h^{\mu}{}_{\mu}$, and the d'Alambertian opereator in flat space is $\Box = \partial_\mu\partial^\mu$.
Contracting again to obtain the Ricci scalar yields

$$\begin{aligned} R &= \frac{1}{2}\big(\partial_\mu\partial^{\nu} h^{\mu}{}_{\nu} - \Box h^{\beta}{}_{\beta} - \partial_\beta\partial^{\beta} h + \partial_\nu\partial^{\mu} h^{\nu}{}_{\mu}\big) \\ &= \partial_\mu\partial_\nu h^{\mu\nu} - \Box h \end{aligned}$$

Therefore the Einstein tensor is

$$G_{\beta\nu} = \frac{1}{2}\big(\partial_\mu\partial_\beta h^{\mu}{}_{\nu} - \Box h_{\beta\nu} - \partial_\nu\partial_\beta h + \partial_\nu\partial^{\mu} h_{\beta\mu} - \eta_{\beta\nu}\partial_\mu\partial_\lambda h^{\mu\lambda} - \eta_{\beta\nu}\Box h\big) \tag{7}$$

If we define the **trace-reversed** perturbation

$$\bar{h}_{\mu\nu} = h_{\mu\nu} - \frac{1}{2}h\eta_{\mu\nu} \qquad\qquad \bar{h} = \bar{h}^{\mu\nu}\eta_{\mu\nu} = -h$$

we can simplify the equation(7). Thus,

$$R_{\beta\nu} = \frac{1}{2}\left(\partial_\mu\partial_\beta\bar{h}^\mu{}_\nu - \Box\bar{h}_{\beta\nu} - \cancel{\partial_\nu\partial_\beta h} + \partial_\nu\partial^\mu\bar{h}_{\beta\mu} + \cancel{\frac{1}{2}\eta_{\nu\mu}\partial^\mu\partial_\beta h} - \frac{1}{2}\eta_{\beta\nu}\Box h + \cancel{\frac{1}{2}\eta_{\beta\mu}\partial_\nu\partial^\mu h}\right)$$

$$= \frac{1}{2}\left(\partial_\mu\partial_\beta\bar{h}^\mu{}_\nu - \Box\bar{h}_{\beta\nu} + \partial_\nu\partial^\mu\bar{h}_{\beta\mu} - \frac{1}{2}\eta_{\beta\nu}\Box h\right)$$

If we contract the above tensor we obtain

$$R = \partial_\mu\partial_\beta\bar{h}^\mu{}_\nu + \frac{1}{2}\eta^{\mu\nu}\partial_\mu\partial_\nu h - \Box h \quad = \partial_\mu\partial_\nu\bar{h}^{\mu\nu} - \frac{1}{2}\Box h$$

So the Einstein's tensor expressed as a function of $\bar{h}_{\mu\nu}$ is

$$G_{\beta\nu} = \frac{1}{2}\left(\partial_\mu\partial_\beta\bar{h}^\mu{}_\nu - \Box\bar{h}_{\beta\nu} + \partial_\nu\partial^\mu\bar{h}_{\beta\mu} - \eta_{\mu\nu}\partial_\mu\partial_\nu\bar{h}^{\mu\nu}\right) \tag{8}$$

This expression can be simplified further by choosing an appropriate gauge transformation. Using the **Lorenz gauge** condition

$$\partial_\mu\bar{h}^{\,\mu\nu} = 0 \tag{9}$$

the Einstein's tensor of equation(8) becomes

$$G_{\beta\nu} = \frac{1}{2}\left(\partial_\beta\partial_\mu\bar{h}^{\mu\alpha}\eta_{\alpha\nu} + \partial_\nu\partial_\mu\bar{h}^{\mu\alpha}\eta_{\alpha\beta} - \eta_{\mu\nu}\partial_\nu\partial_\mu\bar{h}^{\mu\nu} - \Box\bar{h}_{\beta\nu}\right) = -\frac{1}{2}\Box\bar{h}_{\beta\nu}$$

The linearized Einstein's field equation is

$$\Box\bar{h}_{\beta\nu} = -16\pi\, T_{\beta\nu} \tag{10}$$

we will solve the above equation with individual approximations in section(), whereas we work in vacuum. The energy-momentumn tensor $T_{\beta\nu}$ is null in vacuum so the linearized Einstein's equation in vacuum assumes the form of the wave equation in a tensorial form

$$\Box\bar{h}_{\beta\nu} = 0 \tag{11}$$

The above equation shows that the trace-reversed metric perturbation propagate as a wave distorting a flat spacetime.
The simplest solution to the linearized Einstein's equation(11) is a plane wave

$$\bar{h}_{\beta\nu} = A_{\beta\nu}\,\exp\left(i\, k_\alpha x^\alpha\right)$$

where $A_{\beta\nu}$ is called **amplitude tensor** and it is symmetric, since $\bar{h}_{\mu\nu}$ is symmetric.
Substitution of the plane wave solution into equation(11) implies that $k_\alpha k^\alpha = 0$, so k^α is a null four vector. Therefore, the plane wave solution is a gravitational wave which travels at the speed of light in the spatial direction $\mathbf{k} = (k^1, k^2, k^3)/k^0$ and with frequency $\omega = k^0$, i.e. $\bar{h}_{\beta\nu} = A_{\beta\nu}\,\exp\left[i\left(\mathbf{k}\cdot\mathbf{x} - \omega t\right)\right]$. Furthermore, any $\bar{h}_{\mu\nu}$ satisfying the linearized Einstein's field equation(11) in vacuum describes a **gravitational wave** propagating at the speed of light, and it can be Fourier-expanded as a superposition of plane waves.

2.2 Gauge transformations and GW polarizations

A **gauge transformation** in linearized theory is defined as a transformation of the perturbation $h_{\mu\nu}$ into a new metric perturbation $h'_{\mu\nu}$

$$h'_{\mu\nu} = h_{\mu\nu} + \partial_\mu \xi_\nu + \partial_\nu \xi_\mu \tag{12}$$

for a given vector field ξ^μ. Gauge transformations are particularly important because they leave the Riemann curvature tensor unchanged (up to the first order in $h_{\mu\nu}$), indeed, the physical spacetime is unchanged. The invariance of the curvature under such transformations is analogous to the traditional gauge invariance of electromagnetism.
Assuming that the Einstein's field equation(10) are valid everywhere the metric perturbation $h_{\mu\nu}$ contains: gauge degrees of freedom; physical, radiative degrees of freedom; and physical, non-radiative degrees of freedom tied to the matter source of the GW.
It is possible to show that the linearized Einstein's equation can be written as 5 Poisson-type quations, plus a wave equation for the transverse-traceless components of the metric perturbation, which represents the radiative degrees of freedom.
Neverthless this procedure will manifestly demonstrate that the radiative degrees of freedom in spacetime are two, it is a cumbersome and long derivation. Instead, we ignore the degrees of freedom tied to the matter and we consider only solutions of equation(11):

$$\bar{h}_{\mu\nu} = A_{\mu\nu} \exp\left(i\, k_\alpha x^\alpha\right)$$

By using the Lorenz gauge and the transverse traceless gauge, we reduce progressively the number degrees of freedom of a plane wave from 10 to 2.

We want now to find the conditions on the parameter ξ_μ in order to satisfy the Lorenz gauge condition, that we used in the previous section. The initial metric perturbation $h_{\mu\nu}$ tranforms into $h'_{\mu\nu}$ if a gauge transformation is used. However, the new trace reversed metric $\bar{h}'_{\mu\nu}$ transforms as

$$\begin{aligned}
\bar{h}'_{\mu\nu} &= h_{\mu\nu} + \partial_\mu \xi_\nu + \partial_\nu \xi_\mu - \frac{1}{2}\eta_{\mu\nu}\left(h + \partial_\alpha \xi^\alpha + \partial_\alpha \xi^\alpha\right) \\
\bar{h}'_{\mu\nu} &= \bar{h}_{\mu\nu} + \partial_\mu \xi_\nu + \partial_\nu \xi_\mu - \eta_{\mu\nu}\, \partial_\alpha \xi^\alpha
\end{aligned} \tag{13}$$

Imposing the Lorenz gauge $\partial_\mu \bar{h}'^{\,\mu\nu} = \partial_\mu \bar{h}^{\,\mu\nu} = 0$ we obtain

$$\begin{aligned}
\partial_\mu \bar{h}'^{\,\mu\nu} &= \partial_\mu \bar{h}^{\,\mu\nu} + \partial_\mu \partial^\mu \xi^\nu + \partial_\mu \partial^\nu \xi^\mu - \partial_\mu \eta^{\mu\nu}\, \partial_\alpha \xi^\alpha \\
&= 0 + \Box \xi^\nu + \partial^\nu \partial_\mu \xi^\mu - \partial^\nu \partial_\alpha \xi^\alpha = 0
\end{aligned}$$

Any metric perturbation $h_{\mu\nu}$ can therefore be put into a Lorenz gauge by using transformations that satisfy

$$\Box \xi_\mu = 0$$

The plane wave $\xi_\mu = C_\mu \exp[ik_\alpha x^\alpha]$ is a solution of the above equation and it generates a gauge transformation through the four arbitrary constants C_μ.
The **Transverse-Traceless (TT) gauge** is the most convinient gauge for the analysis of the gravitational waves, and it is defined for a plane wave by the following conditions:

a) The Lorenz gauge condition fixes four components of $A_{\mu\nu}$

$$\partial^\mu \bar{h}_{\mu\nu} = A_{\mu\nu} k^\nu = 0$$

The amplitude tensor $A_{\mu\nu}$ and the four vector k^μ are orthogonal.

b) Three components of the aplitude tensor can be eliminated selecting $\xi_\mu = C_\mu \exp[ik_\alpha x^\alpha]$ so that $A^{\mu\nu} u_\mu = 0$ for some chosen four velocity u_μ. Three and not four components are fixed, since one firther constraint $k^\mu A_{\mu\nu} u^\nu$ needs to be satisfied.

c) One component of the aplitude tensor can be eliminated selecting $\xi_\mu = C_\mu \exp[ik_\alpha x^\alpha]$ so that $A^\mu_\mu = 0$.

This means that we have suffecient freedom to fix the values of 8 components of $A_{\mu\nu}$ from a), b) and c), hence, reducing the number of independent component from 10 to 2. Note that $\bar{h}^{\mathrm{TT}}_{\mu\nu} = h^{\mathrm{TT}}_{\mu\nu}$ from c).
What does the TT gauge tell us about gravitational radiation ?
Let use consider a test a particle at rest with four-velocity $u^\alpha = (1, 0, 0, 0)$ in a nearly flat spacetime. If we orient our spatial coordinate axes so that the a plane gravitational wave is travelling in the positive z-direction (equivalentely x^3 direction) $k^\sigma = (\omega, 0, 0, \omega)$ the transverse traceless conditions becomes

$$\left.\begin{aligned} A^{\mathrm{TT}}_{\mu 0}\,\omega + A^{\mathrm{TT}}_{\mu 3}\,\omega = 0 \\ A^{\mathrm{TT}}_{0\nu} = 0 \\ A^{\mathrm{TT}}_{00} + A^{\mathrm{TT}}_{11} + A^{\mathrm{TT}}_{22} + A^{\mathrm{TT}}_{33} = 0 \end{aligned}\right\} \quad \Rightarrow \quad \begin{bmatrix} 0 & 0 & 0 & 0 \\ 0 & A^{\mathrm{TT}}_{11} & A^{\mathrm{TT}}_{12} & 0 \\ 0 & A^{\mathrm{TT}}_{12} & -A^{\mathrm{TT}}_{11} & 0 \\ 0 & 0 & 0 & 0 \end{bmatrix}$$

As a consequence of the transverse traceless gauge the only non-zero component of the metric perturbation $\bar{h}^{\mathrm{TT}}_{\mu\nu}$ are, respectively, the plus $(+)$ and the cross $(\times)$ polarization of the gravitational wave

$$\begin{aligned} \bar{h}^{\mathrm{TT}}_{11} &= -\bar{h}^{\mathrm{TT}}_{22} \equiv h_+ \\ \bar{h}^{\mathrm{TT}}_{12} &= \bar{h}^{\mathrm{TT}}_{21} \equiv h_\times \end{aligned}$$

So, the plane wave solution in the TT gauge is:

$$\bar{h}^{\mathrm{TT}}_{\mu\nu} = \begin{bmatrix} 0 & 0 & 0 & 0 \\ 0 & h_+ & h_\times & 0 \\ 0 & h_\times & -h_+ & 0 \\ 0 & 0 & 0 & 0 \end{bmatrix} \tag{14}$$

where we express the real part of the solution with $x^0 = t$ and $x^3 = z$ as follow

$$h_+ = A_{11}^{\mathrm{TT}} \cos\left(\omega(t-z)\right)$$
$$h_\times = A_{12}^{\mathrm{TT}} \cos\left(\omega(t-z)\right)$$

h_+ and $h_\times$ are the two independent polarizations of a gravitational wave and they completely characterize the gravitational wave solution. We finally found that the radiative degrees of freedom are only two and they are represented by h_+ and $h_\times$.

Generally, within any finite vacuum region it is always possible to find a gauge which is locally transverse and traceless, that is, a guage which satisfies the following general conditions

$$h_{0\nu}^{\mathrm{TT}} = 0$$
$$\eta^{\mu\nu} h_{\mu\nu}^{\mathrm{TT}} = 0$$
$$\partial_\mu h_{\mathrm{TT}}^{\mu\nu} = 0$$

The transverse traceless gauge does not only simplify the expression of the perturbation metric, but it also gives an important relation between the Riemann curvature tensor and the metric perturbation. Since we have already calculated the Riemann curvature tensor in equation(6) we recall the result taking into account the TT gauge conditions

$$\begin{aligned} R^{\mu}{}_{00\sigma} &= \frac{1}{2}\left(\partial_0\partial_0 h^{\mathrm{TT}\mu}{}_{\sigma} - \partial_0\partial^\mu h_{0\sigma}^{\mathrm{TT}} - \partial_\sigma\partial_0 h^{\mathrm{TT}\,\mu}{}_{0} + \partial_\sigma\partial^\mu h_{00}^{\mathrm{TT}}\right) \\ &= \frac{1}{2}\partial_0\partial_0 h^{\mathrm{TT}\mu}{}_{\sigma} \qquad\qquad \text{using } h_{\mu 0}^{\mathrm{TT}} = 0 \end{aligned} \tag{15}$$

The above result tells us that the curvature of spacetime is proportional to the 'acceleration' of the gravitational wave. Considering a plane wave we have

$$R^{\mu}{}_{00\sigma} = -\frac{1}{2}\omega^2 A^{\mathrm{TT}\mu}{}_{\sigma} \cos(\omega(t-z))$$

where ω is the frequency of the plane wave. The curvature is proportional to the square of the frequency, in fact we expect a bigger curvature if the wave oscillates more times per second. Neverthless we considered the simple model of a plane wave, we can say, naively, that the spacetime is more curved if the ripples of the GW are squeezed in a narrow time interval. Analogously, the electromagnetic field of an oscillating electric dipole is proportional to the square of the frequency, in fact we expect a more intense field if the charge oscillates more times per second.

3 Effects of Gravitational Waves

We have shown how the gravitational waves are obtained from the Einstein's field equation. By using the transverse traceless gauge we introduced crucial semplifications. We want now to explain the important physical consequences of the theoretical results obtained in the previous part. Throughout the next sections we will use the linearized theory of gravitatinal waves and we consider our metric to be in the TT gauge.

3.1 Free particles and detection principles

In general relativity the trajectory of a free falling particle is described by the **geodesic equation**

$$\frac{\mathrm{d}^2 x^\beta}{\mathrm{d}\tau^2} + \Gamma^\beta{}_{\mu\nu} \frac{\mathrm{d}x^\mu}{\mathrm{d}\tau} \frac{\mathrm{d}x^\nu}{\mathrm{d}\tau} = 0 \tag{16}$$

where the coordinates of the particle are represented x^β and τ is the proper time.
We choose a frame in which a test particle is initially at rest, i.e. with initial four-velocity

$$u^\mu = \frac{\mathrm{d}x^\mu}{\mathrm{d}\tau} = (1, 0, 0, 0)$$

We consider a plane wave in the TT gauge propagating towards the test particle.
Equation(16) can be used to express the initial acceleration of the particle

$$\left(\frac{\mathrm{d}u^\beta}{\mathrm{d}\tau}\right)_0 = -\Gamma^\beta{}_{00} = -\frac{1}{2}\eta^{\beta\alpha}(\partial_0 h_{\alpha 0} + \partial_0 h_{0\alpha} + \partial_\alpha h_{00})$$

However, we recall from the TT gauge that

$$h^{\mathrm{TT}}_{0\alpha} = 0 \qquad\qquad h^{\mathrm{TT}}_{\mu\nu} = \bar{h}^{\mathrm{TT}}_{\mu\nu}$$

for all α. Hence, the initial acceleration of the particle is zero and a free particle, initally at rest, will remain at rest indefinitely.
In this constext "being at rest" means that the coordinates of the particle do not change, so the TT gauge is a good choice of coordinate. As the gravitational waves propagates, the coordinate system moves with the ripples of the spacetime, in order to keep the particle in the initial position.
In the TT gauge free falling bodies are not influenced by GWs, and their coordinate separation is constant. However, the proper separation is not constant, so let us calculate it.
Consider two free falling test particles located at $z = 0$ and separated on the x axis by a coordinate distance L_c. We still consider a plane wave in the TT gauge propagating in

the z direction.
The proper distance between the particles is

$$\begin{aligned} L &= \int_0^{L_c} |g_{\mu\nu}\,\mathrm{d}x^\mu \mathrm{d}x^\nu|^{1/2} = \int_0^{L_c} \sqrt{g_{11}}\mathrm{d}x = \int_0^{L_c} \sqrt{1+h_+(t,z=0)}\mathrm{d}x \\ &\approx \int_0^{L_c} \left(1+\frac{1}{2}h_+(t,z=0)\right)\mathrm{d}x = L_c\left(1+\frac{1}{2}h_+(t,z=0)\right) \end{aligned}$$

If we had considered two particles on the y axis separated by the same coordinate distance, the proper distance would have been

$$L \approx L_c\left(1-\frac{1}{2}h_+(t,z=0)\right)$$

Therefore, recalling the expression of the plus polarization for a plane wave

$$h_+ = A_{11}^{\mathrm{TT}} \cos\left(\omega(t-z)\right)$$

we notice that the particles along x axis are streched, whereas the particles along the y axis are squeezed.
The proper distance is streched by the passing gravitational wave and the two particles oscillate with a fractional length change given by

$$\frac{\delta L}{L} \approx \frac{1}{2}h_+(t,z=0) \tag{17}$$

The proper distance is a very important quantity which has a crucial experimental use. For instance, a laser interferometer gravitational wave detector consists of four masses that hang from vibration-isolated supports as shown in Figure(1). When a gravitational wave passes through the detector, it changes the arm-length difference, thereby an optical system monitors the separations between the masses in such a way that the variations in the output of the photodiode are directly proportional to δL. The value of ΔL is a composition of the two polarizations of the gravitational wave h_+ and $h_\times$, and it also contains terms that weigh the direction of the GW. One adjusts the reflectivities of the interferometers corner mirrors such that a typical photon travles up and down the cavity of order 100 times before returning to the beamsplitter and being directed into the photodiode. So, the accumulated phase shift in each arm will be

$$\delta\phi \sim 100\frac{4\pi\delta L}{\lambda}$$

where λ is the wavelength and δL is the distance the mirror moves relative to the beam splitter. This phase shift can be measured at the photodiode to an accuracy that is governed by the lights photon shot noise $\sim 1/\sqrt{N}$, where N is the number of photons that enter the interferometer from the laser.

Laser interferometer gravitational wave detector

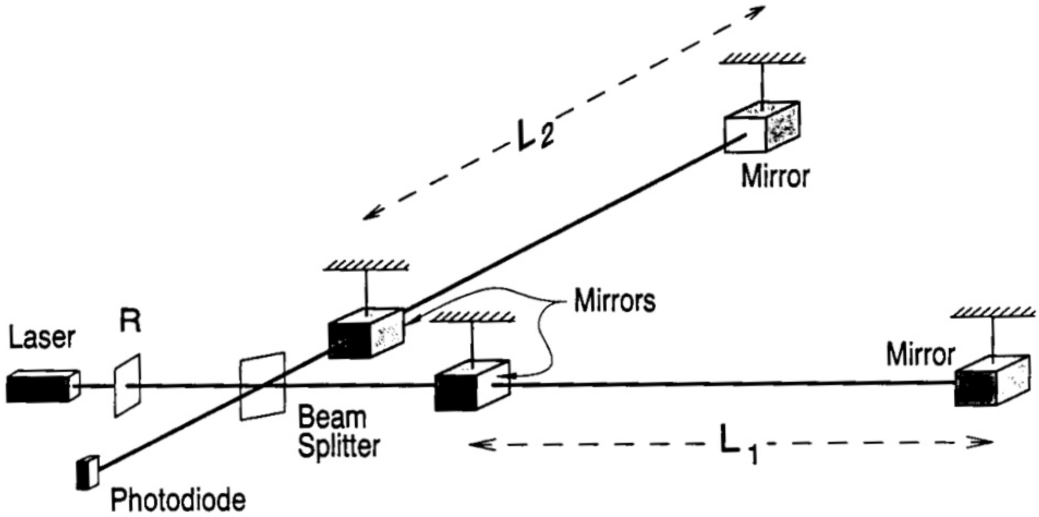

Figure 1: Schematic representation of a laser interferomenter gravitational wave detector (from REF).

3.2 From the geodesic deviation equation to the + and × polarizations

Since free-falling bodies obey to the geodesic equation(16), in this section we study the physical effects of the two polarizations plus + and times × of the gravitational waves through relative motions of geodesics.
The **geodesic deviation equation** expresses the relative acceleration between two neighboring geodesics belonging to a one-parameter geodesics $\gamma_s(\tau)$:

$$\frac{D^2}{d\tau^2} S^\mu = R^\mu{}_{\nu\rho\sigma} T^\nu T^\rho S^\sigma \tag{18}$$

where $S^\mu = \partial x^\mu / \partial s$ is the deviattion from the geodesic, $T^\nu = \partial x^\mu / \partial \tau$ is the tangent to the geodesic and the directional covariant derivative is

$$\frac{D}{d\tau} = \frac{\mathrm{d}x^\mu}{\mathrm{d}\tau} \nabla_\mu$$

A non-zero acceleration of the deviation bewteen between neighbouring geodesics is a signature of spacetime curvature. In fact, geodesic deviation cannot distinguish between a zero gravitational field and a uniform grabitational field. Only tidal gravitational fields give rise to an acceleration in the geodesic deviation.

Let us consider some nearby particles with four-velocities described by a single vector field u^μ and separation vector field S^μ, the geodesic deviation equation(18) becomes

$$\frac{D^2}{d\tau^2}S^\mu = R^\mu{}_{\nu\rho\sigma}\, u^\nu u^\rho S^\sigma \tag{19}$$

The four-velocity vector can be approximated with a unit vector in the time direction plus corrections of order $h^{\mathrm{TT}}_{\mu\nu}$ and higher, however the Reimann curvature tensor is already first order. Therefore, we ignore the corrections of the four-velocity vector and we approximate $u^\nu = (1,0,0,0)$.
Since we have already calculated the Riemann curvature tensor in equation(15) taking into account the TT gauge conditions we recall the result

$$R^\mu{}_{00\sigma} \;=\; \frac{1}{2}\partial_0\partial_0 h^{\mathrm{TT}\mu}{}_\sigma$$

In the lowest order approximation the free-falling particles are slowly moving, then we have $\tau = x^0 = t$, so the geodesic deviation equation becomes

$$\frac{\partial^2}{\partial t^2}S^\mu = \frac{1}{2}S^\sigma\frac{\partial^2}{\partial t^2}h^{\mathrm{TT}\mu}{}_\sigma \tag{20}$$

The above equation is a set of differential equations that can be rewritten using the two polarizations of the metric perturbation (equation(14))

$$\begin{aligned}\frac{\partial^2}{\partial t^2}S^1 &= \frac{1}{2}S^1\frac{\partial^2}{\partial t^2}h_+ + \frac{1}{2}S^2\frac{\partial^2}{\partial t^2}h_\times\\ \frac{\partial^2}{\partial t^2}S^2 &= \frac{1}{2}S^1\frac{\partial^2}{\partial t^2}h_\times - \frac{1}{2}S^2\frac{\partial^2}{\partial t^2}h_+\end{aligned}$$

These can be solved to yield, to lowest order,

$$S^1 = S^1(t=0)\left(1+\frac{1}{2}h_+\right) + \frac{1}{2}h_\times S^2(t=0)$$

$$S^2 = S^2(t=0)\left(1-\frac{1}{2}h_+\right) + \frac{1}{2}h_\times S^1(t=0)$$

Let us study the effects of the two polarizations h_+ and $h_\times$ of a gravitational wave, which propagates through the center of a ring of free-falling test particles. So, let us use consider a plane wave travelling along the z axis, and let us place a ring of free-falling test particles on the x-y plane with its center in $(0,0,0)$. The ring is initially parametrized by $(\cos\theta, \sin\theta)$ with $\theta \in (0, 2\pi]$ and the separation vector S^μ measures the deformation of the ring from its center.

Beginning with the case $h_\times = 0$ and $h_+ \neq 0$, the solutions of the geodesic deviation

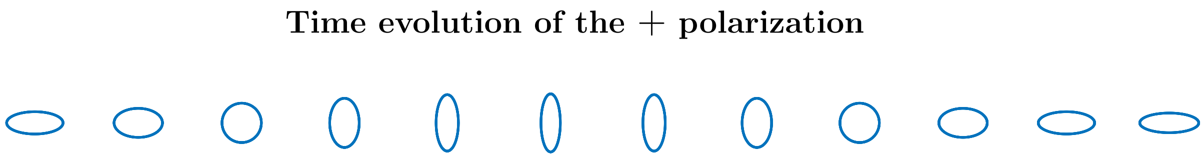

Figure 2: Effect of the h_+ mode on a ring of free-falling test particles at $\omega t = n\pi/6$ with $n = 0, ..., 12$.

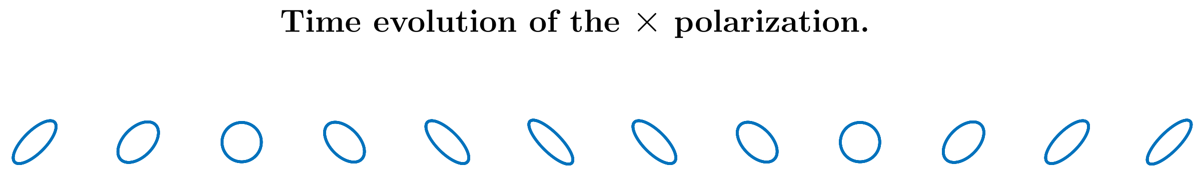

Figure 3: Effect of the $h_\times$ mode on a ring of free-falling test particles at $\omega t = n\pi/6$ with $n = 0, ..., 12$.

equation are

$$S^1_+ = \cos\theta\left(1 + \frac{1}{2}A^{\mathrm{TT}}_{11}\cos(\omega t)\right) \tag{21}$$

$$S^2_+ = \sin\theta\left(1 - \frac{1}{2}A^{\mathrm{TT}}_{11}\cos(\omega t)\right) \tag{22}$$

where $h_+ = A^{\mathrm{TT}}_{11}\cos(\omega t)$ for a plane wave. The time evolution of the ring is shown in Figure(2).

When the plus polarized gravitational wave propagates through the ring, it increases the proper distance between the ring and its center along the x axis when the phase of the wave is close to $\omega t = 0, 2\pi$, meanwhile it squeezes the test particles along the y axis. If the phase of the gravitational wave is close to $\omega t = \pi/2, 3\pi/2$ the ring is stretched along the y axis and the test particles move inwards, therefore, the proper distance from the center of the ring is reduced. As the wave passes, the test particles bounce back and forth in the shape of + as shown in Figure(5a).

On the ohter hand, the case where $h_\times \neq 0$ and $h_+ = 0$ yields the geodesic deviation solutions to be

$$S^1_\times = \cos\theta + \frac{1}{2}\sin\theta A^{\mathrm{TT}}_{12}\cos(\omega t)$$

$$S^2_\times = \sin\theta + \frac{1}{2}\cos\theta A^{\mathrm{TT}}_{12}\cos(\omega t)$$

where $h_\times = A^{\mathrm{TT}}_{12}\cos(\omega t)$ for a plane wave. The relationship between these solutions and those for $h_+ \neq 0$ can be easily found if we rotate the x and y axis through an angle of

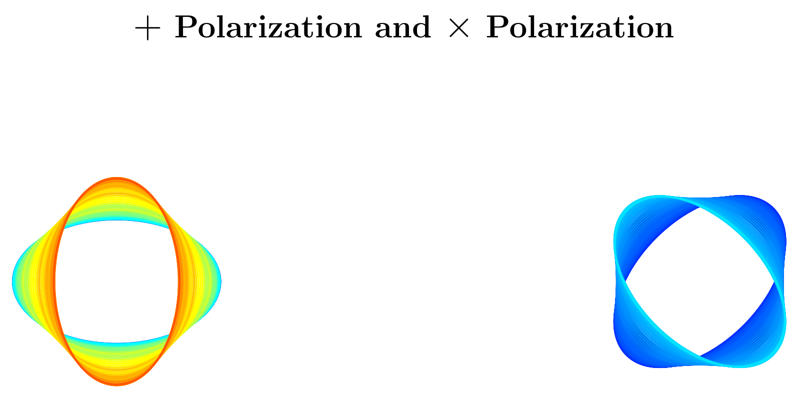

(a) + polarized gravitational wave. (b) × polarized gravitational wave.

Figure 4: Spatial positions occupied by a ring of free-falling test particles disturbed by a gravitational wave.

$-\pi/4$, so that the new coordinate axis are

$$x' = \frac{1}{\sqrt{2}}(x - y)$$

$$y' = \frac{1}{\sqrt{2}}(x + y)$$

Then, the geodesic deviations S_+ of equations (21) and (22) with $h_+ \neq 0$ and $h_\times = 0$ become

$$S'^{\,1}_+ = (S^1_+ - S^2_+)/\sqrt{2} = \cos(\theta + \pi/4) + \frac{1}{2}\sin(\theta + \pi/4)h_+$$

$$S'^{\,2}_+ = (S^1_+ + S^2_+)/\sqrt{2} = \sin(\theta + \pi/4) + \frac{1}{2}\cos(\theta + \pi/4)h_+$$

The above equations are similiar to those with $h_+ = 0$ and $h_\times \neq 0$, in fact the deviations $S^1_\times$ and $S^2_\times$ are nothing but the plus polarization rotated of an angle $-\pi/4$. So, in this case ($h_+ = 0$ and $h_\times \neq 0$) the circle of particles bounce back and forth in the shape of $\times$ as we can see from Figures (3) and (5b). We could consider also right- and left-handed cricularly polarized modes by defining

$$h_R = \frac{1}{\sqrt{2}}(h_+ - ih_\times) \tag{23}$$

$$h_L = \frac{1}{\sqrt{2}}(h_+ + ih_\times) \tag{24}$$

Right- and Left-handed cricularly polarized modes

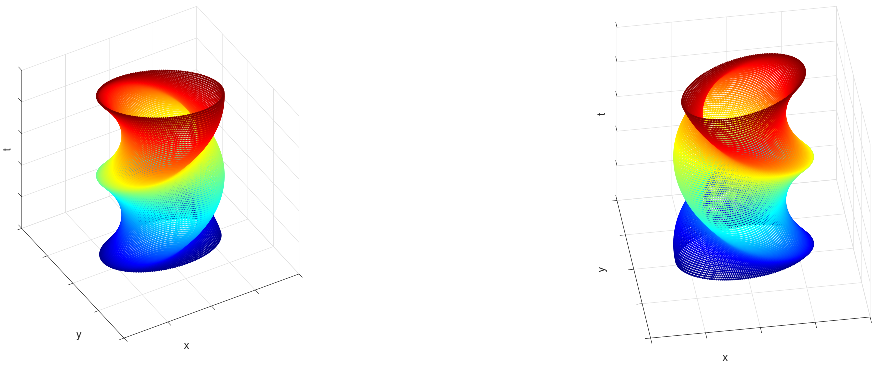

(a) Right-handed polarized gravitational wave.

(b) Left-handed polarized gravitational wave.

Figure 5: Time evoluition of a ring of free-falling test particles on the x-y plane.

The effect of a pure h_R wave would be to rotate the particles in a right-handed sense and similiarly for the left-handed mode h_L. It is important to stress that the particles do not travel around the ring, they just move in little epicycles.

Another remarkable consequence of the plus $+$ and times $\times$ polarizations is that it is possible to relate the polarization states of classical gravitational waves to the kinds of particles we would expect to find upon quantization. The spin of a quantized field is directly realted to the transformation properties of that field under spatial rotations. For instance, the electromagnetic field has two independent polarization states, which can be described by vectors in the x-y plane, and they are invariant under a rotation by 360°. Upon quantization, the theory yields the photon, a massless spin-1 particle. The general rule is that the spin s is related to the angle θ under which the polarization modes are in invariant by $s = 360°/\theta$. Since the gravitational field, whose waves propagate at the speed of light with polarizartion states invariant under rotations of 180°, should lead to a massless spin-2 particle: the graviton. Despite the fact that we are a long way from detecting such particles, any possible quantum theory of gravity should predict their existence with these properties.

4 Production of Gravitational Waves

We have studied how the gravitational waves propagate in vacuum. We now want to understand the relation between the gravitational waves and their source. In most of the physical scenarios the system that produces the gravitational waves is small compared to the distances with the detector. Therefore, in order to study the solutions of the linearized Einstein's field equation(10) we make a crucial approximation

4.1 Solution of the linearized Einstein's field equation

The generation of gravitational radiation depends on the movements of objects in space-time. So far, we have neglected the presence of matter and we solved the linearized Einstein's field equation in vacuum. However, if we want to analyze the relation between sources and gravitational waves we need to consider $T_{\mu\nu} \neq 0$ and solve equation(10):

$$\Box \bar{h}_{\mu\nu} = -16\pi \, T_{\mu\nu}$$

It is possible to solve this equation using a Green function $G(x^\sigma - y^\sigma)$, such that

$$\Box_x G(x^\sigma - y^\sigma) = \delta^{(4)}(x^\sigma - y^\sigma) \tag{25}$$

And the general solution is, then, given by

$$\bar{h}_{\mu\nu}(x^\sigma) = -16\pi \int G(x^\sigma - y^\sigma) T_{\mu\nu}(y^\sigma) \, \mathrm{d}^4 y \tag{26}$$

$$\Box_x \bar{h}_{\mu\nu}(x^\sigma) = -16\pi \int \Box_x G(x^\sigma - y^\sigma) T_{\mu\nu}(y^\sigma) \, \mathrm{d}^4 y = -16\pi \, T_{\mu\nu}(x^\sigma)$$

There are two solutions of equation(25): one solution represents a wave travelling forward in time and, the other represents a wave travelling backward in time. The two solutions are called, respectively, retarded and advanced. We are interested in the **retarded Green function**, which represents the accumulated effect of signals received at (x^0, x^1, x^2, x^3) from a source at (y^0, y^1, y^2, y^3):

$$G(x^\sigma - y^\sigma) = -\frac{1}{4\pi |\mathbf{x} - \mathbf{y}|} \, \delta\left[|\mathbf{x} - \mathbf{y}| - (x^0 - y^0)\right] \theta(x^0 - y^0)$$

where have used boldface to denote the patial vectors $\mathbf{x} = (x^1, x^2, x^3)$ and $\mathbf{y} = (y^1, y^2, y^3)$, with norm $|\mathbf{x} - \mathbf{y}| = \left[\delta_{ij}(x^i - y^i)(x^j - y^j)\right]^{1/2}$. The Heaviside step function $\theta(x^0 - y^0)$ is 1 when $x^0 > y^0$, and zero otherwise.

Plugging the retarded Green function into equation(26) and integrating on the y^0 coordinate we obtain

$$\bar{h}_{\mu\nu}(t, \mathbf{x}) = 4 \int \frac{1}{|\mathbf{x} - \mathbf{y}|} T_{\mu\nu}(t - |\mathbf{x} - \mathbf{y}|, \mathbf{y}) \, \mathrm{d}^3 y \tag{27}$$

where $t = x^0$ and the integration is made over the spatial coordinates. From equation(27) we notice that the metric perturbation is influenced by the matter and energy distribution, $T_{\mu\nu}$, at time $t - |\mathbf{x} - \mathbf{y}|$. Since the gravitational radiation travels at the speed of light $c = 1$, the metric perturbation at $(t, \mathbf{x})$ is influenced by the radiation that was produced by the source at the retarded time $t_r = t - |\mathbf{x} - \mathbf{y}|$.
We have obtained a general solution, however it possible to derive a formula that reaveals the quadrupole nature of the gravitational radiation if we assume:

- **far field approximation**: the metric perturbation (27) is evaluated at large distances from the source

$$|\mathbf{x} - \mathbf{y}| \approx |x| \equiv r \tag{28}$$

  The fractional error of this approximation scales as $\sim L/r$, where L is the size of the source.

- **slowly moving source**: the light traverses the source much faster than the components of the cource itself do. Therefore, the source moves at non relativistic speeds.

- **isolated system**: the source of the gravitational radiation is an isolated and compact. We assume that our system and the radiation are not gravitationally influenced by other bodies.

So we rewrite equation(27) using the far field approximation:

$$\bar{h}_{\mu\nu}(t, \mathbf{x}) = \frac{4}{r} \int T_{\mu\nu}(t - r, \mathbf{y}) \, \mathrm{d}^3 y$$

Since most of the sources are very far from the detection point, the above result is a very good approximation in most of the cases, and it shows the $1/r$ dependency of the gravitational wave.
Using the Fourier transform and inverse with respect to time

$$\begin{aligned} \phi(t, \mathbf{x}) &= \mathcal{F}^{-1}[\tilde{\phi}(\omega, \mathbf{x})] \equiv \frac{1}{\sqrt{2\pi}} \int \mathrm{d}\omega e^{-i\omega t} \tilde{\phi}(\omega, \mathbf{x}) \\ \tilde{\phi}(\omega, \mathbf{x}) &= \mathcal{F}[\phi(t, \mathbf{x})] \equiv \frac{1}{\sqrt{2\pi}} \int \mathrm{d}t e^{i\omega t} \phi(\omega, \mathbf{x}) \end{aligned}$$

applied to the metric perturbation

$$\begin{aligned}
\mathscr{H}_{\mu\nu}(\omega,t) &\equiv \mathcal{F}[\bar{h}_{\mu\nu}(t,\mathbf{x})] = \frac{1}{\sqrt{2\pi}}\int e^{i\omega t}\bar{h}_{\mu\nu}(t,\mathbf{x})\ \mathrm{d}t \\
&= \frac{4}{\sqrt{2\pi}}\int e^{i\omega t}\frac{T_{\mu\nu}(t_r,\mathbf{y})}{r}\ \mathrm{d}t\,\mathrm{d}^3y \\
&= \frac{4}{\sqrt{2\pi}\,r}\int e^{i\omega(t_r+r)}\,T_{\mu\nu}(t_r,\mathbf{y})\ \mathrm{d}t_r\,\mathrm{d}^3y \\
&= \frac{4\,e^{i\omega r}}{r}\int \mathscr{T}_{\mu\nu}(\omega,\mathbf{y})\ \mathrm{d}^3y
\end{aligned} \tag{29}$$

where we used a change of variable and we defined the Fourier transform of the energy momentum tensor as $\mathscr{T}_{\mu\nu} \equiv \mathcal{F}[T_{\mu\nu}]$.
The Lorenz gauge condition $\partial_\mu \bar{h}^{\mu\nu} = 0$ in the Fourier space becomes

$$\mathcal{F}\left[\partial_0\bar{h}^{0\nu} + \partial_j\bar{h}^{j\nu}\right] = 0$$

$$\mathscr{H}^{0\nu} = \frac{i}{\omega}\partial_j\mathscr{H}^{j\nu}$$

As a consequence, we only need to calculate the spacelike components $\mathscr{H}^{j\nu}$. We set $\nu = k$ in order to find $\mathscr{H}^{0k}$ from $\mathscr{H}^{jk}$, afterwards we use $\mathscr{H}^{k0}$ to get h^{00}. The integration by parts of the spacelike components of equation(29) is

$$\int \mathscr{T}^{jk}\mathrm{d}^3y = \int \partial_m\left(\mathscr{T}^{mk}y^j\right)\mathrm{d}^3y - \int \partial_m\left(\mathscr{T}^{mk}\right)y^j\mathrm{d}^3y$$

Since we assumed that the source is isolated, the first term, which is a surface integral, vanishes. Whereas, the conservation of the energy-momentum tensor $\partial_\mu T^{\mu\nu} = 0$ yields in the Fourier space

$$-\partial_m\left(\mathscr{T}^{mk}\right) = i\omega\mathscr{T}^{0k}$$

Notice that the conservation of the energy-momentum tensor is a very strong assumption, because the motion of bodies is governed by non-gravitational interactions. However, and remarkably, the result depends only on the sources motion and not on the forces acting on them. Thus,

$$
\begin{aligned}
\int \mathscr{T}^{jk}(\omega,\mathbf{y})\mathrm{d}^3y &= i\omega\int y^j\,\mathscr{T}^{0k}\;\mathrm{d}^3y \\
\text{symmetry of } \mathscr{T}_{k\nu}\rightarrow &= \frac{i\omega}{2}\int\left(y^j\,\mathscr{T}^{0k}+y^k\,\mathscr{T}^{0j}\right)\mathrm{d}^3y \\
\partial_l\left(y^ky^j\,\mathscr{T}^{0l}\right)=\delta^k_l y^j\,\mathscr{T}^{0l}+\delta^j_l y^k\,\mathscr{T}^{0l}+y^ky^j\partial_l\mathscr{T}^{0l}\rightarrow &= \frac{i\omega}{2}\int\left[\partial_l\left(y^ky^j\,\mathscr{T}^{0l}\right)-y^ky^j\partial_l\mathscr{T}^{0l}\right]\mathrm{d}^3y \\
\partial_l\mathscr{T}^{0l}=\partial_l\mathscr{T}^{l0}=-i\omega\mathscr{T}^{00}\rightarrow &= -\frac{\omega^2}{2}\int y^ky^j\,\mathscr{T}^{00}(\omega,\mathbf{y})\;\mathrm{d}^3y
\end{aligned}
$$

Then, equation(29) becomes

$$
\begin{aligned}
\mathscr{H}_{kj} &= -\frac{4\,e^{i\omega r}}{r}\frac{\omega^2}{2}\int y^ky^j\,\mathscr{T}^{00}(\omega,\mathbf{y})\;\mathrm{d}^3y \\
\mathcal{F}\left[\frac{\partial^2T^{00}}{\partial t^2}\right]=-\omega^2\mathcal{F}[T^{00}]\rightarrow &= \frac{2}{r}\int y^ky^j\mathcal{F}\left[\frac{\partial^2}{\partial t^2}T^{00}(t_r,\mathbf{y})\right]\;\mathrm{d}^3y \\
&= \mathcal{F}\left[\frac{2}{r}\frac{\partial^2}{\partial t^2}\left(\int y^ky^jT^{00}(t_r,\mathbf{y})\;\mathrm{d}^3y\right)\right]
\end{aligned}
$$

We can transform back the above result to obtain the original metric perturbation

$$
\bar{h}_{kj}=\frac{2}{r}\frac{\mathrm{d}^2}{\mathrm{d}t^2}I_{kj}(t_r) \tag{30}
$$

where we defined the **quadrupole moment tensor**

$$
I_{kj}(t)=\int y_ky_jT^{00}(t,\mathbf{y})\;\mathrm{d}^3y \tag{31}
$$

To complete the derivation we need to express the metric perturbation in the TT gauge, so we must make the right hand side of equation(30) traceless and transverse.
We begin by introducing the spatial projection tensor

$$
P_{ij}=\delta_{ij}-n_in_j \tag{32}
$$

which projects the components of a tensor (with rank 2) into a surface orthogonal to the unit vector n^i

$$
(P_{ij}X^{il})n^j=X^{jl}n_j-n_in_jX^{il}n^j=0
$$

We can us the **projection tensor** to construct the transverse-traceless version of a symmetric spatial tensor X_{ij} via

$$
X^{TT}_{ij}=\left(P_i^{\,k}P_j^{\,l}-\frac{1}{2}P_{ij}P^{kl}\right)X_{kl} \tag{33}
$$

where the first and second terms make the tensor, respectively, transverse and tracless. In addition, we define the **reduced quadrupole moment tensor** as

$$\mathcal{I}_{kj} = I_{kj} - \frac{1}{3}\delta_{kj} I \qquad\qquad \text{where } I = \eta^{lm} I_{lm} = I^m_m \tag{34}$$

which is traceless, and, for $T^{00} = \rho$, it assume the expression

$$\mathcal{I}_{kj} = \int \rho(\mathbf{y}) \left(y_k y_j - \frac{1}{3}\delta_{kj} y^l y_l \right) \mathrm{d}^3 y$$

We now have all the concepts to write down the **quadrupole formula**

$$h^{\mathrm{TT}}_{ij} = \frac{2}{r} \frac{\mathrm{d}^2 \mathcal{I}_{kl}(t_r)}{\mathrm{d}t^2} \left(P_i^k P_j^l - \frac{1}{2} P_{ij} P^{kl} \right) \tag{35}$$

which represents the metric perturbation of equation(30) in the TT gauge, since $h^{\mathrm{TT}}_{\mu\nu} = \bar{h}^{\mathrm{TT}}_{\mu\nu}$. Notice that the gravitational wave scales as $\sim 1/r$.

4.2 The nature of the gravitational radiation

The quadrupole formula (35) and its derivation gives a first insight into the properties of the gravitational waves and their sources.
Firstly, the gravitational radiation has a **quadrupolar nature**, because the GW produced by an isolated nonrelativisitc object is proportional to the second derivative of the reduced quadrupole moment of the energy density. It is possible to justify qualitatively the quadrupole nature, defining the gravitational analogue of the dipole moment: **mass dipole moment**

$$\mathbf{D} = \sum_i m_i \mathbf{x}_i \tag{36}$$

where the m_i is the rest mass and $\mathbf{x}_i$ is the spatial postion of particle i.
The leading contribution to the electromagnetic radiation comes from the changing dipole moment. However, the first derivative of the mass dipole moment is the total linear momentum

$$\frac{\mathrm{d}\mathbf{D}}{\mathrm{d}t} = \sum_i m_i \frac{\mathrm{d}\mathbf{x}_i}{\mathrm{d}t} = \mathbf{p}$$

Since the total linear momentum is conserved, there can be no mass dipole radiation from any source.
Similiarly, the gravitational analogue of the magnetic dipole moment is

$$\mu = \sum_i \mathbf{x}_i \times \left(m_i \frac{\mathrm{d}\mathbf{x}_i}{\mathrm{d}t} \right) = \mathbf{J}$$

where $\mathbf{J}$ is the total angular momentum of the system. Since the total angular momentum is conserved. Hence, there can be no dipole radiation of any sort from a gravitational source. It should be stressed that for a spherical distribution of matter (or energy) the quadrupole moment is a constant, even if the body is rotating: thus, a spherical star does not emit gravitational waves.
We now study the GW-emission of a binary system in circular orbit with radius R. We assume that two equal-mass stars are orbiting far from each others with an angular frequency ω and they can be trated as point particles on the $x^1 - x^2$ plane. Thus,

$$T^{00}(t,\mathbf{x}) = M\delta(x^3)\big[\delta\big(x^1 - R\cos\omega t\big)\delta\big(x^2 - R\sin\omega t\big) + \delta\big(x^1 + R\cos\omega t\big)\delta\big(x^2 + R\sin\omega t\big)\big]$$

The motion of the system is studied using the Newtonian approximations, so using the Kepler third law we obtain the link between the angular frequency and the radius of the orbit:

$$\omega^2 a^3 = M_T G \qquad \rightarrow \qquad \omega = \left(\frac{M}{4R^3}\right)^{1/2}$$

where we used as total mass of the system $M_T = 2M$, semi-major axis $a = 2R$ and $G = 1$. The quadrupole moment tensor (31) becomes

$$I_{ij}(t) = 2MR^2 \begin{bmatrix} \cos^2\omega t & \cos\omega t\sin\omega t & 0 \\ \cos\omega t\sin\omega t & \sin^2\omega t & 0 \\ 0 & 0 & 0 \end{bmatrix}$$

Then, the reduced quadrupole moment (34) is easily found to be

$$\mathcal{I}_{ij}(t) = 2MR^2 \begin{bmatrix} \cos^2\omega t - 1/3 & \cos\omega t\sin\omega t & 0 \\ \cos\omega t\sin\omega t & \sin^2\omega t - 1/3 & 0 \\ 0 & 0 & -1/3 \end{bmatrix}$$

Taking the second derivative of the above tensor and using the projection tensor with $n_j = \delta_{j3} \rightarrow \mathbf{n} = (0,0,1)$:

$$P_{jk} = \delta_{jk} - n_j n_k$$

we obtain the gravitational wave through the the quadrupole formula(35):

$$h_{ij}^{\mathrm{TT}} = \frac{8\,GM\,R^2\omega^2}{c^4\,r} \begin{bmatrix} -\cos 2\omega t & -\sin 2\omega t & 0 \\ \sin 2\omega t & \cos 2\omega t & 0 \\ 0 & 0 & 0 \end{bmatrix}$$

where we inserted G and c in order to give an estimates of the coefficient.
Two remarkable aspects of the above formula are that the gravitational radiation is emitted at twice the angular frequency at which the system rotates, and $h_+^{\mathrm{TT}} = ih_\times^{\mathrm{TT}}$ so the wave is circularly polarized.
We will see again these aspects when we will treat the numerical simulations, but let us now give an order-of-magnitude estimate of the amplitude of the gravitational wave

$$\mathcal{H} = \frac{8\,GM\,R^2\omega^2}{c^4\,r}$$

We assume that the two objects to be separated by a distance R equal three times their Schwarzschild radii $r_s = 2GM/c^2$. In addition we consider that the two objects have approximately the mass of the Sun $M = M_{\odot} = 2 \times 10^{30}$kg and they rotate with an angular frequency given by the Kepler's third law $\omega = \sqrt{GM/(4R^3)}$.

$$\frac{G}{c^4} = 8.26 \times 10^{-45} \mathrm{kg}^{-1}\,\mathrm{s}^2\mathrm{m}^{-1}$$

$$r_s = 2.95 \times 10^3\,\mathrm{m}$$

$$R = 3r_s = 8.86 \times 10^3\,\mathrm{m}$$

$$\omega = 6.9 \times 10^3 \mathrm{s}^{-1}$$

Pluging into $\mathcal{H}$ and considering the source at the a cosmological distance $r = 100\,\mathrm{M}pc \approx 3.09 \times 10^{24}$m we have

$$\mathcal{H} = 1.6 \times 10^{-22}$$

Altough we used Newtonian formulae in a regime where the GR becomes to be important, we obtained an estimate of the gravitational wave amplitude.
Taking into account the discussion we made in section(3.1), if an interferometer of length $L = 4\,\mathrm{km}$ was affected by a gravitational wave with intensity $\langle$, the streething in the arm-length would be of order

$$\delta L = L\,\mathcal{H} = 6.38 \times 10^{-19}\,\mathrm{m}$$

and the laser light with wavelength $\lambda = 10^{-6}$m would acquire a phase shift

$$\delta\phi = 100\frac{4\pi}{\lambda}\delta L = 8.02 \times 10^{-10}$$

5 Numerical Evolution of Compact Binaries

In the linearized approximation, where gravitational fields are weak and velocities are nonrelativistic, we showed that it is straightforward to derive a relationship between the matter dynamics and the emission of gravitational waves, thus obtaining the quadrupole formula. However, the strongest gravitational-wave signals come from highly compact systems that evolve at relativistic speeds, where the linearized assumptions do not apply. Therefore, gravitational-wave detectors find more likely an event which has a powreful signals. Thus, it is important to be able to calculate gravitational-wave emission accurately for processes such as black hole or neutron star inspiral and merger. Such problems cannot be solved analytically and instead are modeled by numerical relativity to compute the gravitational field near the source.
In this section we study the gravitational-wave signals obtained from numerical simulations of compact binaries, using the Einstein Toolkit, an open-source computational infrastructure for numerical relativity based on Cactus Framework.
The Cactus framework [ref] is a general framework for the development of portable, modular applications, wherein programs are split into components (called thorns) with clearly defined dependencies and interactions. Thorns are typically developed independently and do not directly interact with each other. Cactus simulations require an executable to be compiled, and this executable has one mandatory argument: a parameter file. The parameter file is a simple text file, containing the desired settings within the simulation, it is used not only to set up the initial conditions and the necessary thorns for the simulation, but also to choose outputs and their format.
A thorough description of the numerical methods used to perform the simulations can be found here, we depict the initial conditions of our simulations and we briefly mention the used thorns. Rather than analyzing the algorithms of th Einstein Toolkit, the purpose of the following sections is to study the gravitational-wave signals of binaries black holes (BBH) and neutron stars (BNS).

5.1 Gravitational Wave Extraction

Using `WeylScal4`, the Einstein Toolkit calculates the Newman-Penrose scalar ψ_4 (also called Weyl scalar 4)[REF], which is linked to the GW strain by the following relation, valid only at spatial infinity:

$$\psi_4 = \frac{\partial^2}{\partial t^2}(h_+ - ih_\times) \tag{37}$$

In order for equation(37) to be valid, the signal has to be extracted as furthest as possible from the source. The signal is then decomposed in spin-weighted spherical harmonics of spin -2 by the thorn `Multipole` []

$$\psi_4(t',r,\theta,\phi) = \sum_{l=2}^{\infty} \sum_{m=-l}^{l=2} \psi_4^{lm}(t',r)\, {}_{-2}Y_{lm}(\theta,\phi)$$

The output given by the Einstein Toolkit is therefore $\psi_4^{lm}(t',r)$, however, in this work we only focus on the dominant $l = m = 2$ mode and we get the GW strain form following a procedure similiar to REFSince $\psi_4^{lm}(t',r)$ is extracted at a distance r from the source center, our data detect the signal at a time t', which is different from the instant when the radiation was emitted. So, we subtract from the output time t' the distance from the source r in order to compute the gravitational radiation as if the signal would have been emitted at the coordinate origin.
We are interested in the behavior of the gravitational wave at a given time and distance $(t,r) = (t'-r,r)$, so we neglect the numerical factor ${}_{-2}Y_{lm}(\theta,\phi)$ given by choosing an arbitrary angle (θ,ϕ) for the spin-weighted spherical harmonics. Thus, we integrate twice in time in order to get the complex-valued gravitational strain

$$\tilde{h}(t) = \int_0^t \int_0^{\hat{t}} \psi_4^{2,2}(t^*,r)\,\mathrm{d}t^*\,\mathrm{d}\hat{t}$$

where we used the trapezodail rule for the numeric integration. The resulting quantity obtained with the procedure described above show a left-over non-linear drift, which can be eliminated performing a fit to a second order polynomial for both the real and the imaginary parts of $\tilde{h}(t)$. The two polarizations (plus and times) of the gravitational wave are finally obtained subtracting the noise

$$h_+(t) = \mathrm{Re}\Big\{\tilde{h}\Big\} - \big(Q_0^R + Q_1^R t + Q_2^R t^2\big) \tag{38}$$

$$h_\times(t) = -\Big[\mathrm{Im}\Big\{\tilde{h}\Big\} - \big(Q_0^I + Q_1^I t + Q_2^I t^2\big)\Big] \tag{39}$$

where the Q values are the coefficients of the fitted polynomials for the real Q^R and the imaginary Q^I parts of $\tilde{h}(t)$.
As we have seen in section(4.1) the gravitational radiation scales with the distance from the source as $1/r$. Therefore, in order to have an order of magnitude of the **gravitational wave strain**

$$h(t) = h_+ - ih_\times \tag{40}$$

where h_+ and $h_\times$ are taken from equations(38) and (39), we multiply $h(t)$ by the distance at which it is was measured and we divide it by a typical cosmological distance of binary sources $r = 100\,\mathrm{Mpc} \approx 3.1\times10^{19}\,\mathrm{km}$. In addition, the units of time will be expressed in millisecond in order to easily compare the frequency of the signals with the sensitivities of the gravitational wave detetctors.

simulation name	par_b	par_m_plus	par_P_plus[1]
BBH-b3	3	0.47656	+0.13808
BBH-b4	4	0.48243	+0.11148
BBH-b5	5	0.48595	+0.095433
BBH-b6	6	0.48830	+0.084541
BBH-b7	7	0.48997	+0.076578
BBH-b10	10	0.49299	+0.061542

Table 1: The table shows the quasi-equilibrium initial conditions used in the `TwoPuncture` thorn. Since the two balck holes have equal masses `par_m_plus`=`par_m_minus` and opposite momentum `par_P_plus[1]`$= -$`par_P_minus[1]`, we do not report in the table the obvious initial conditions of the second black hole.

5.2 Binary Black Hole

As we have done so far and following the Einstein Tookit conventions, we set $G = c = 1$, and therefore we express time and space in units of solar masses $M_\odot$, i.e. $1t[M_\odot] \approx 0.005$ms and $1x[M_\odot] \approx 1.5$km.
We simulate the evolution of equal-mass binary black holes with different quasi-equilirbium initial conditions. The thorn `TwoPunctures` is used to set up the initial data for the two black holes located at the x-axis with opposite linear momentum along the y-axis. Due to the symmetry of the problem, it is possible to reduce the computational cost by a factor of 2 by not evolving the domain with $z < 0$, and by another factor 2 evolving points with $x > 0$ and populating the missing part by rotating the existing domain for 180 degrees along the z-axis. An example of initial data set in the parameter file is

```
TwoPunctures::par_b = 3.0
TwoPunctures::par_m_plus = 0.47656
TwoPunctures::par_m_minus = 0.47656
TwoPunctures::par_P_plus [1] = +0.13808
TwoPunctures::par_P_minus[1] = -0.13808
```

We call parameter b the parameter `par_b` which defines the initial distance of the two black holes at $(x, y, z) = (\pm 3, 0, 0)$ from the origin of the axes. `par_m_plus` and `par_m_minus` set the "bare mass" parameter, and `par_P_plus[1]` and `par_P_minus[1]` set the Bowen-York linear momentum parameter. We let evolve the binary black hole using six different quasi-equilibrium initial conditions, as shown in Table(1). Each initial configuration is then evolved using the `ML_BSSN` (`McLachlan` BSSN) thorn, the gravitational wave information is extracted using `WeylScal4` thorn.
The orbits of covered by the binaries black hole are shown in Figure(6). Due to the short initial distance from the origin, the BBHs with a with low b merge after few revolutions, for instance BBH-b3 merges after 2 revolutions; BBH-b4 merges after 3.5 revolutions; BBH-b5 merges after 6 revolutions. Whereas the BBHs with an high parameter$b$ have

Orbits of different configurations of BBH

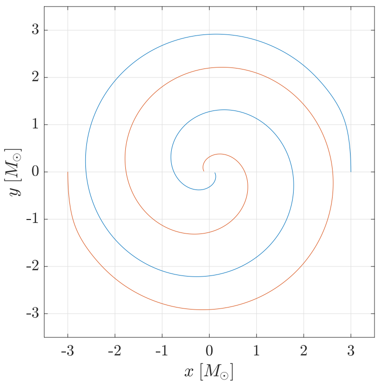

(a) Trajectory of the BBH with initial distance from the origin $b = 3\,M_\odot$.

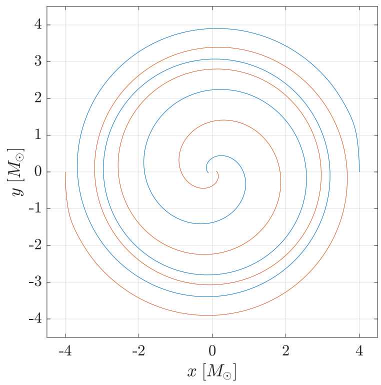

(b) Trajectory of the BBH with initial distance from the origin $b = 4\,M_\odot$.

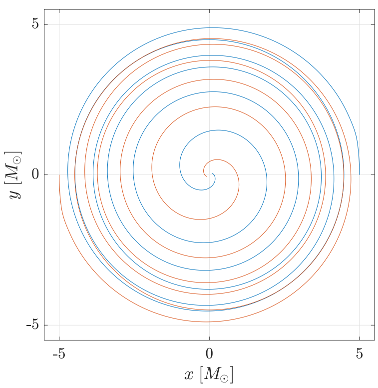

(c) Trajectory of the BBH with initial distance from the origin $b = 5\,M_\odot$.

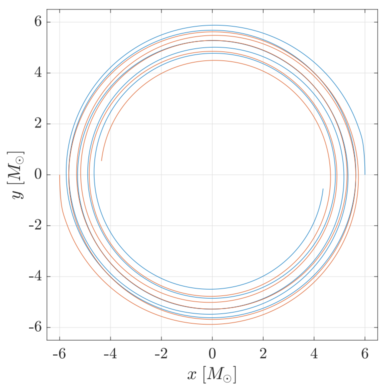

(d) Trajectory of the BBH with initial distance from the origin $b = 6\,M_\odot$.

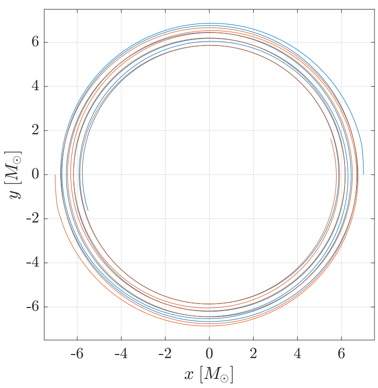

(e) Trajectory of the BBH with initial distance from the origin $b = 7\,M_\odot$.

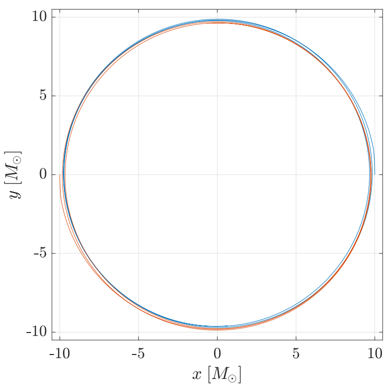

(f) Trajectory of the BBH with initial distance from the origin $b = 10\,M_\odot$.

Figure 6: It is shown the evolution of the BBH using the quasi-equilibrium initial conditions of Table(1). As the parameter b increases, the orbits of the BBH tend to be more stable, where with stable we mean that the difference between the previous and the next orbit is small.

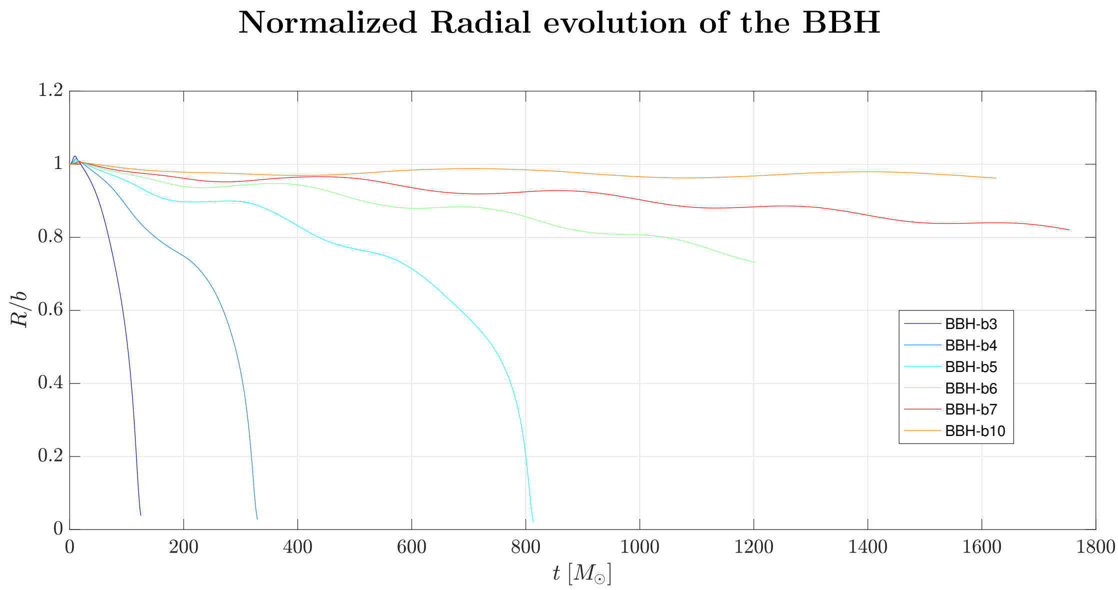

Figure 7: Time evolution of the distance $R(t)$ between a black hole and the origin of the axes. The values are normalized to the initial separation from the origin b. The figure shows oscillation modes especially for BBHs with high b.

orbits close to each other, such that they form a ring shape.
Notice that as the b increases, the two black holes have orbits that drift apart from the coil-shaped path of Figure(6a). This behavior can be better understood analyzing the distance of one of the balck hole from the origin as a function of time. For this reason, we plot in Figure(7) the normalized radial distance

$$R(t)/b = \frac{\sqrt{x^2(t) + y^2(t)}}{b}$$

which depicts a new feature of the orbits. There are evident oscillations of the time-evolution of the radius $R(t)$.

We now study the gravitational radiation emitted by the different binary sources is extracted following to the procedure described in section(5.1).
The gravitational singals are shown in Figure(8), (9), (10), (11), (12) and (13). In the time interval $t \in (0, 0.1)$ms the gravitational wave of all simulations ψ_4 shows an irregular perturbation. In [REF] it is pointed out that there is a numerical noise that could be reduced using a more refined simulations. However, the simulations are enough accurate for our purpose after that time interval.

Gravitational Wave emitted by BBH-b3

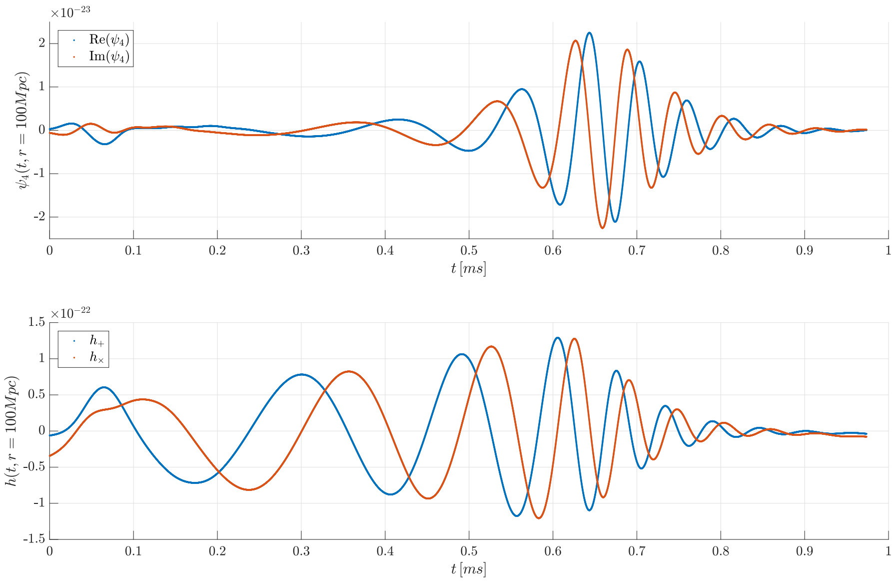

Figure 8: The first and the second panels show, respectively the gravitational signal $\psi_4 = \psi_4^{2,2}$ and the gravitational strain produced by the BBH-b3.

Gravitational waves emitted by BBH-b4

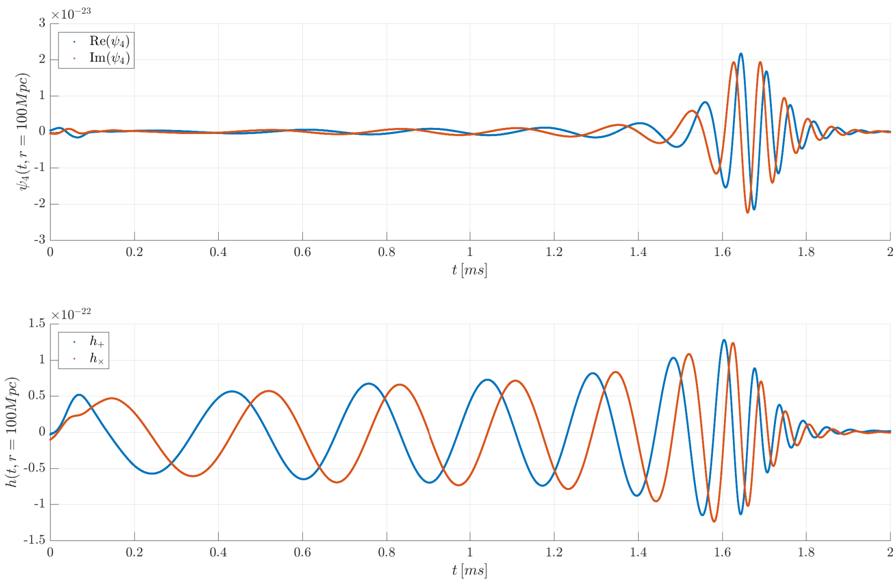

Figure 9: The first and the second panels show, respectively the gravitational signal $\psi_4 = \psi_4^{2,2}$ and the gravitational strain produced by the BBH-b4.

Gravitational waves emitted by BBH-b5

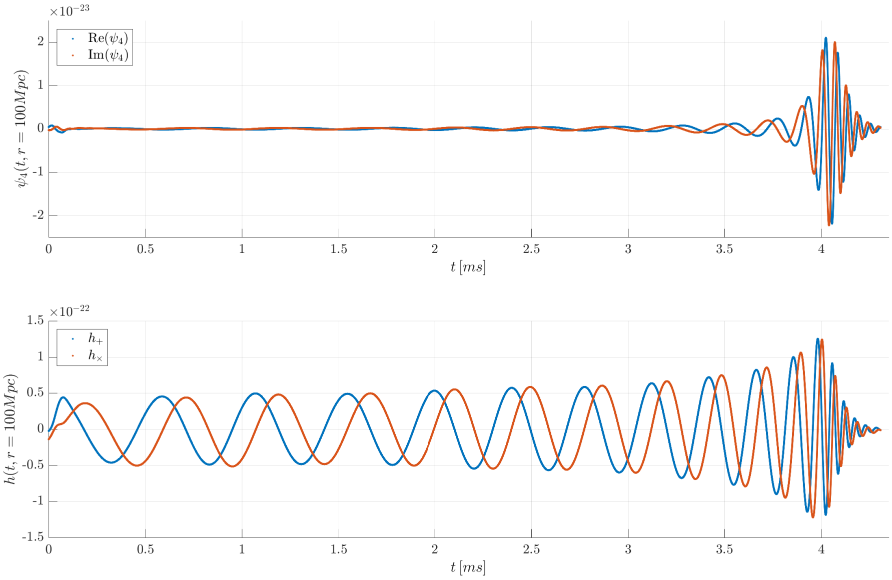

Figure 10: The first and the second panels show, respectively the gravitational signal $\psi_4 = \psi_4^{2,2}$ and the gravitational strain produced by the BBH-b5.

The GW radiated by the binary black hole with parameter $b = 3$, in Figure(8), has a short duration with respect to the others due to the intial conditions. In fact, due to the strong interaction between the two bodies, the black holes merge quickly after $125\, M_\odot \approx 0.616\,\mathrm{ms}$ from Figure(7). The radius of the orbit decreases rapidly and the inspiralling phase lasts only 0.6ms and, as a consequence the waveform is a sinusoid with a noticeable varying frequency. After 6.1ms the gravitational wave aplitude starts decreasing and oscillating around zero as expected in the ring-down phase, in which the black holes are already merged.
The gravitational radiations emitted of BBH-b4 and BBH-b5 are pretty similiar, they both show the typical phase of insipralling that can be approximated with a sinusoid analogue to the quadrupole formula. Since the BBH-b5 has a initial configuration with further initial separation than BBH-b4, the signal of BBH-b5 lasts longer 4.5ms than the GW radiaition of BBH-b4 lasting 2ms.
The gravitational strains h of BBH-b3, BBH-b4 and BBH-b5 have similiar amplitudes, the strain increases its vale from $\approx 0.5 \times 10^{-22}$ up to $\approx 1.5 \times 10^{-22}$ during the inspiralling, and the ring-doww phase lasts approximately 0.5 ms.
The gravitational signal ψ_4 radiated by the BBH-b6 source has big initial noise and it is affected by perturbations between $(1, 1.5)$ms. Alothough the gravitational strain h will be affected by this perturbations, its oscillation modes in Figure(11) are rather smooth. In a time interval of 5ms the amplitudes of the two polarizations h_+ and $h_\times$ vary, respectively, from 3.9×10^{-23} to 5×10^{-23}, and from 3×10^{-23} up t 4.5×10^{-23}. These small variations

shows similiar features with the quadrupole formula approximation, which could roughly describe the inspiralling phase.
As expected, by increasing the parameter b, the gravitational strain decreases in intensity in the first part of the black hole evolution. The ψ_4 signals produced by BBH-b7 and BBH-b10 have noises analogue to those of BBH-b6, however they manifest a new feature in the gravitational strain h. Indeed, it is evident from Figures (13) and (12) that the two polarization h_+ and $h_\times$ have another oscillation mode with larger period that the typical sinusoidal oscillation mode.
The consequence of such behavior could be due to a rough numerical exctraction, or to the oscillations in the radial distance from the center in Figure(7).
As a matter of fact, the waveform that can be better approximated using our rudimentary methods of analysis is that on of BBH-b6.

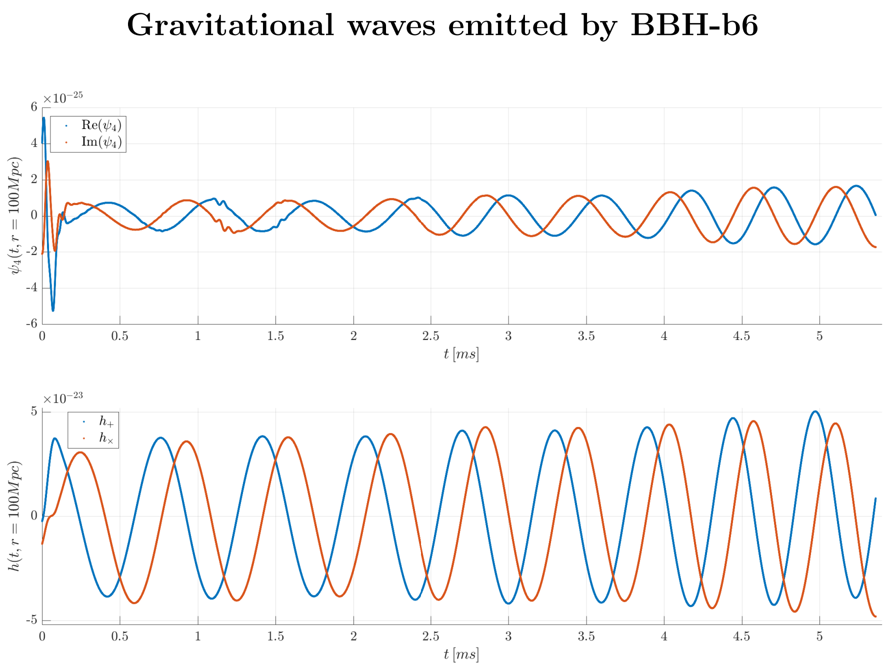

Figure 11: The first and the second panels show, respectively the gravitational signal $\psi_4 = \psi_4^{2,2}$ and the gravitational strain produced by the BBH-b6.

Gravitational waves emitted by BBH-b7

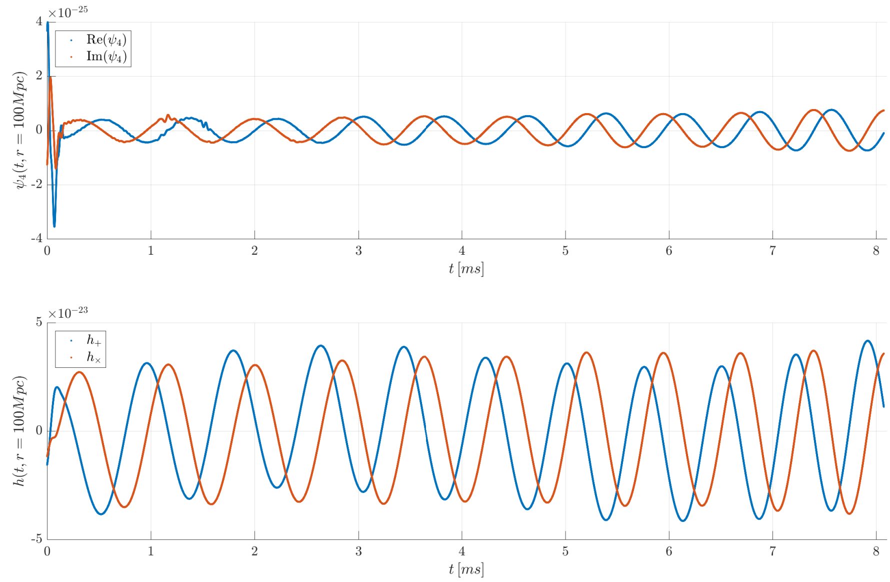

Figure 12: The first and the second panels show, respectively the gravitational signal $\psi_4 = \psi_4^{2,2}$ and the gravitational strain produced by the BBH-b7.

Gravitational waves emitted by BBH-b10

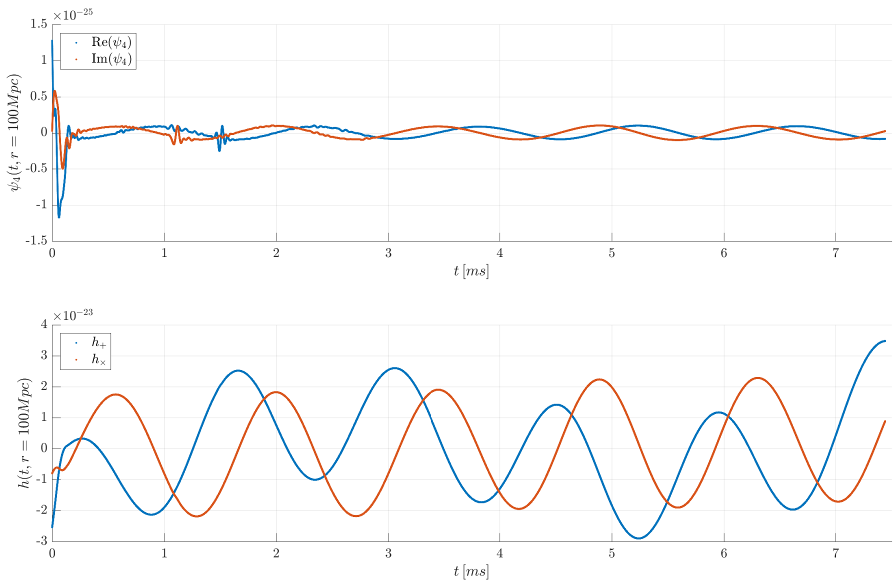

Figure 13: The first and the second panels show, respectively the gravitational signal $\psi_4 = \psi_4^{2,2}$ and the gravitational strain produced by the BBH-b10.

An important result obtained through the quadrupole formula applied to a binary source was that the frequency of the gravitational wave is twice the orbital frequency of rotating bodies. Using the Fourier transform of the gravitational strain and the angular frequency data of the black holes we can test this hypothesis.

We plot in Figures (14) and (15),on the left side, the normalized absolute value of the Fourier transform of the gravitational wave strain:

$$|\mathcal{F}[h(t, r = 100\,Mpc)]| = \left| \frac{\int e^{i\omega t} h(t, r = 100\,Mpc)\ \mathrm{d}t}{\max\left[\int e^{i\omega t} h(t, r = 100\,Mpc)\ \mathrm{d}t\right]} \right|$$

and on the right side the angular velocity of the BBHs:

$$\omega = \frac{x\,v_y - y\,v_x}{x^2 + y^2}$$

where x and y are the coordinates of one of the BH, whereas v_x and v_y are the velocities along respectively the x and y axis.
Figures (14b), (14d) and (14f) show that the orbital angular velocity increases more rapidly for higher values of b in the last milli seconds of the simulation. This aspect cannot be seen from Figures (15b), (15d) and (15f), because the simulations do not last enough for the black holes to merge. However, the angular velocities of BBH-b6, BBH-b7, BBH-b10 manifest the typical oscillations that we have also noticed in the previous discussions.
The Fourier transform allows us to study the range of angular frequencies of the GWs. In Figures (14a), (14c) and (14e) it is evident a peak on an angular frequency that is approximately twice the mean value of the orbital angular frequencies of the rotating black in Figures (14b), (14d) and (14f). Notice that the peak is more narrow for higher values of b, since the initial sinusoidal behavior of the gravitational wave is more evident and longer for simulations with high b.
The BBH-b6, BBH-b7 and BBH-b10 depict, as well, the typical peak at twice the orbital angular frequency. We confirm that the gravitational wave strain of a binary balck holes source such has an angular frequency at twice the orbital angular frequency of the rotating bodies.
Although the peaks are particularly sharp, each Figure (15a), (15c) and (15e) manifest a smaller peak at lower frequencies, which has an increasing intensity with the increasing parameter b. Such phenomenon could be due to the oscillations of the BBH orbits, however, a more accurate analysis is needed to confirm this hypothesis.

Fourier transforms of the gravitational strain $\mathcal{F}[h](\omega)$ and orbital angular velocities ω of BBH-b3, BBH-b4 and BBH-b5

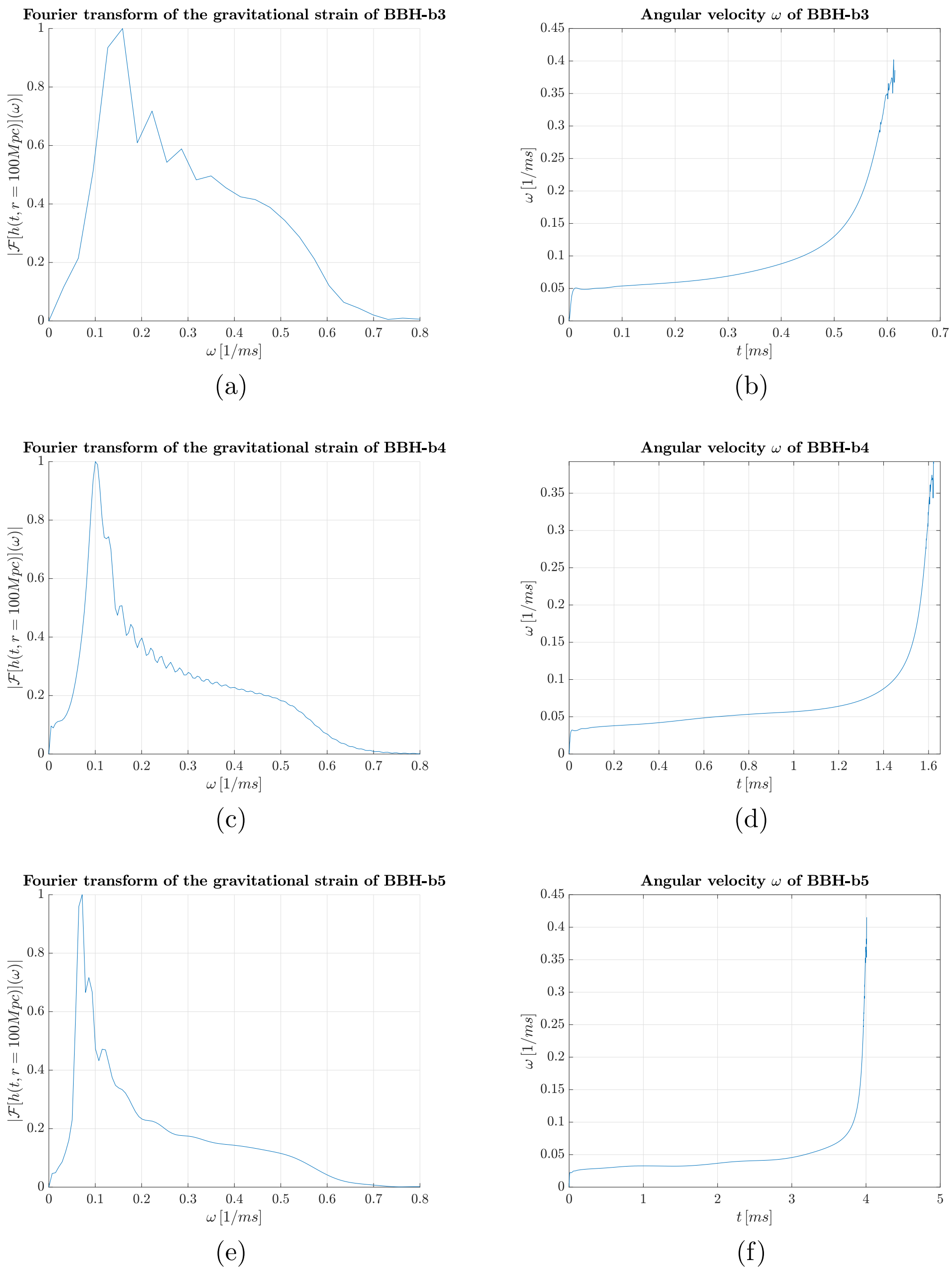

Figure 14: The Figures hows the absolute value of normalized Fourier transform of $h(t)$ and the orbital angular velocities ω of the different binaries. The Fourier transform has a peak approximately on the mean value of the orbital angular velocity, which confirms the theoretical prediction given by the quadrupole formula.

Fourier transforms of the gravitational strain $\mathcal{F}[h](\omega)$ and orbital angular velocities ω of the BBH-b6, BBH-b7 and BBH-b10

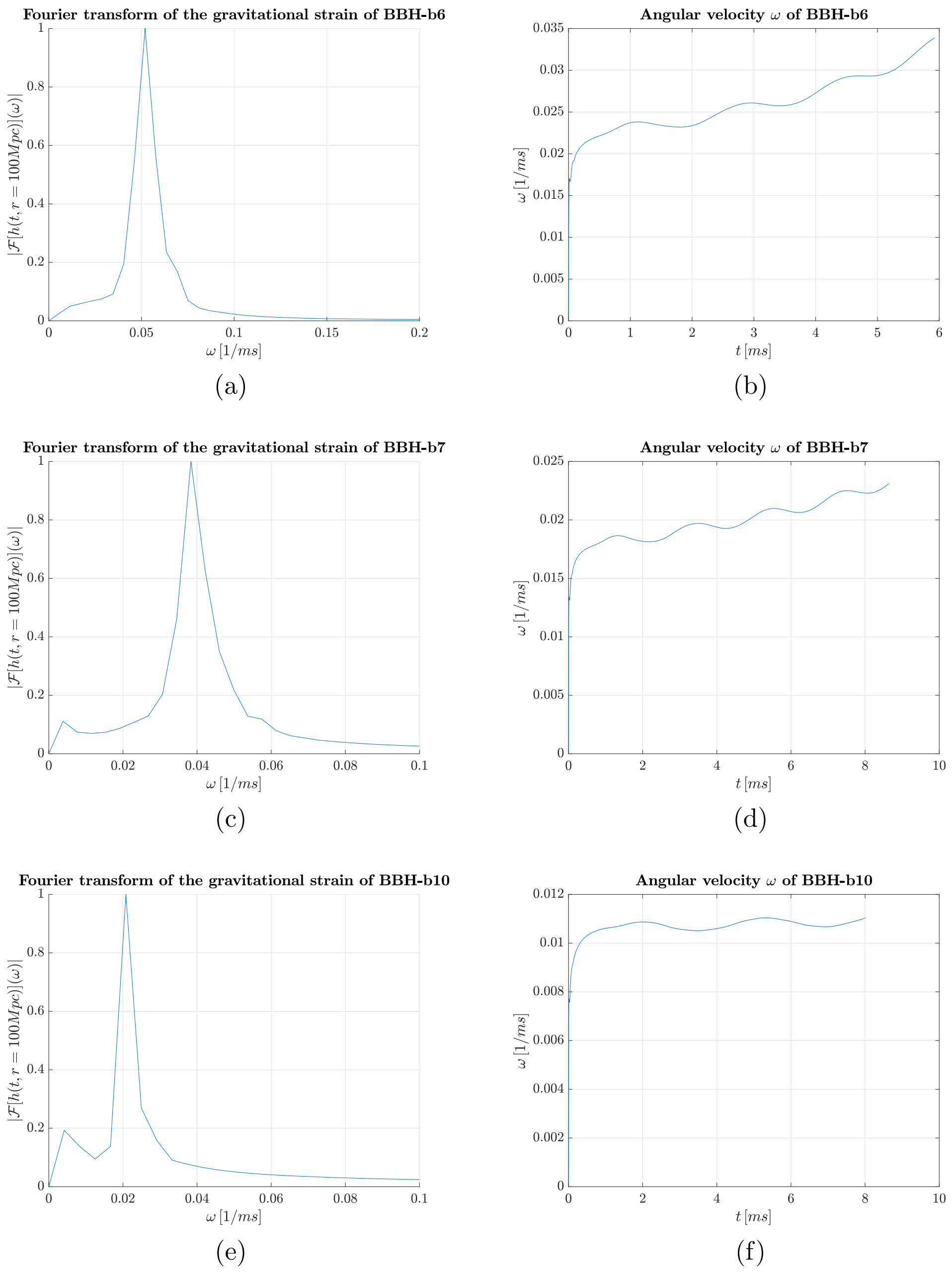

Figure 15: The Figures hows the absolute value of normalized Fourier transform of $h(t)$ and the angular velocities of the different binaries. The Fourier transform has a peak approximately on the mean value of the orbital angular velocity, which confirms the theoretical prediction given by the quadrupole formula.

5.3 Binary Neutron Star

We now study the evolution of a binary neutron star (BNS) made of two equal-mass objects rotating with an quasi-equilibrium initial conditions obtained using the software `Lorene` [REF]. The total ADM mass of the system is $M_{\mathrm{ADM}} = 3.251\, M_{\odot}$. Since the two neutron stars are placed at in symmetric initial conditions with respect to the z axis, as in the binary black holes, the problem has a π symmetry that reduces the computational cost. The hydrodynamics evolution of the neutron stars is achieved using the ideal fluid approximation. The link between pressure P and density ρ is provided by the following equation of state (EOS)

$$P = K\, \rho^{\Gamma}$$

where K is the polytropic constant and Γ is the adiabatic index.
The initial separation between the two neutron stars is set to be $45\,\mathrm{km} \approx 30.47\, M_{\odot}$, whereas we set $K = 123.6$ and $\Gamma = 2$.

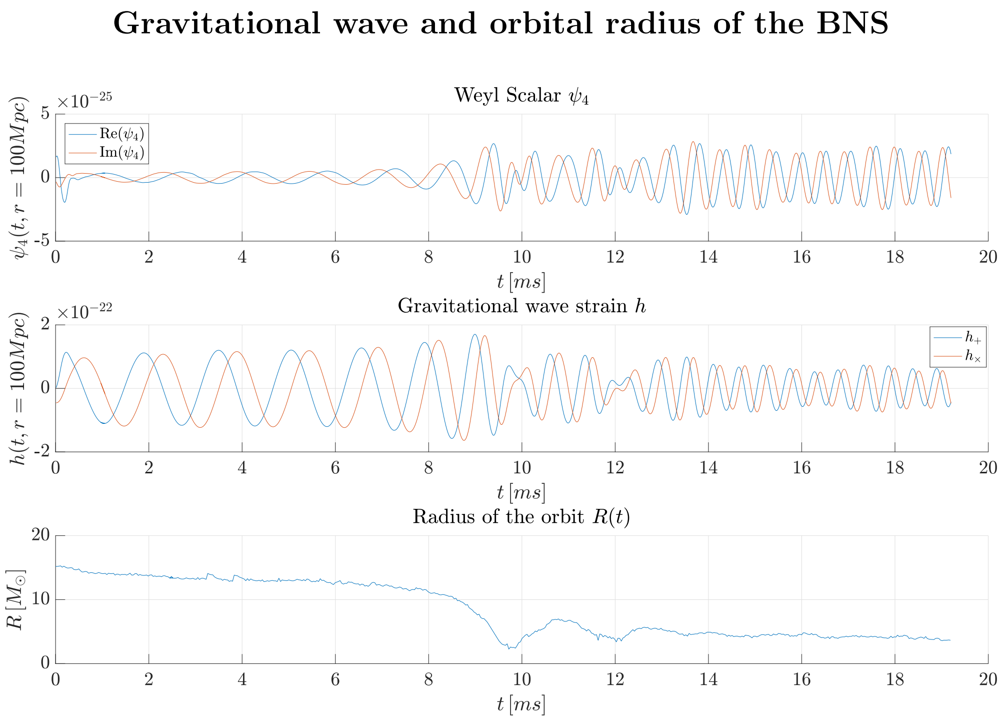

Figure 16: The first and the second panels show, respectively the gravitational signal $\psi_4 = \psi_4^{2,2}$ produced by the BNS, whereas the third pane shows the orbital radius obtained defined as the highest value of the density. Notice the bouncing behavior after $t \approx 9$ms, when the stars start bouncing and the gravitational wave decreases slowly its amplitude.

The gravitational wave strain h is extracted following the procedure in section(5.1),

whereas the orbital radius R is obtained calculating the highest value of density ρ at each time step.
The gravitational wave and the orbital radius are shown in Figure(16). During the inspiralling phase $t \in (0, 8.5)$ ms, the gravitational wave is similiar to that one of the binary black holes, indeed, BNS and BBH both show a sinusoid with an increasing frequency. However, when the strain reaches the highest value approximately at $t \approx 9$ms, the signal does not drop off as rapidly as for the black holes one, but it rebounds while slowly decreasing. The orbital radius R shows an analogue behavior, in fact, it reaches the lowest value right at $t \approx 9.9$ms and then it oscillates aroud $R \approx 4\, M_{\odot}$.
The reason of such behavior relies on the differences between a black hole and a neutron star. However, since we could not continue simulations for a longer time, we cannot describe the features of the wave form in detail, but we speculate on the expected outcome and discuss the significance of the wave forms from the observational point of view. Due to the nature of balck holes, the ring-down phase is short because when the events of horizon are enough close, the black holes merge into single black hole which shrinks quickly. So, the gravitational waveform amplitude of the BHs damps rapidly after the merger.
In general, massive objects such neutron stars could collapse under their own weight forming a black hole depending on the compactness of the neutron stars before the merger.[REF]If this happens, the gravitational wave strain manifests a ring-down phase similiar to that one of the binary black holes. In our case, we speculate that the binary neutron stars do not form a black hole, because they are not enough compact and they transfer matter between themselves and outwards.
In order to analyze the matter distribution during the simulation, let us study the rest mass density during the time evolution of the BNS.
In Figure (17) it is shown the intial stage of the BNS evolution. From Figure(17a) it is possible to notice how the gravitational attraction between the two objects slighlty reshapes their surfaces. After $t = 3.83\text{ms} = 777.6\, M_{\odot}$ the stars start tranfering matter between themselves, meanwhile a stream of matter is being ejected (Figure(17c)).
When the gravitational strain reaches the highest amplitude ≈ 9ms, the neutron stars have a prolate shape (Figure(17d)). Instead of merging, the matter bounces off again and again during the final stage of the evolution Figure(18). Such behavior and the high rotational velocity lead the system to eject a big amount of matter, during the ring-down phase (Figures(18a) and (18b)). The matter, that does not overcome the "centrifugal force", is thrown away in a spiralling shape.
The gravitational wave strain contains crucial information about the evoltuion of a system, indeed, it can give a clue on the matter evolution of our binary system. As Thorn would say "gravitational waves will show us details of the bulk motion of dense concentrations of energy".[REF]

Initial stage of the rest mass density evolution

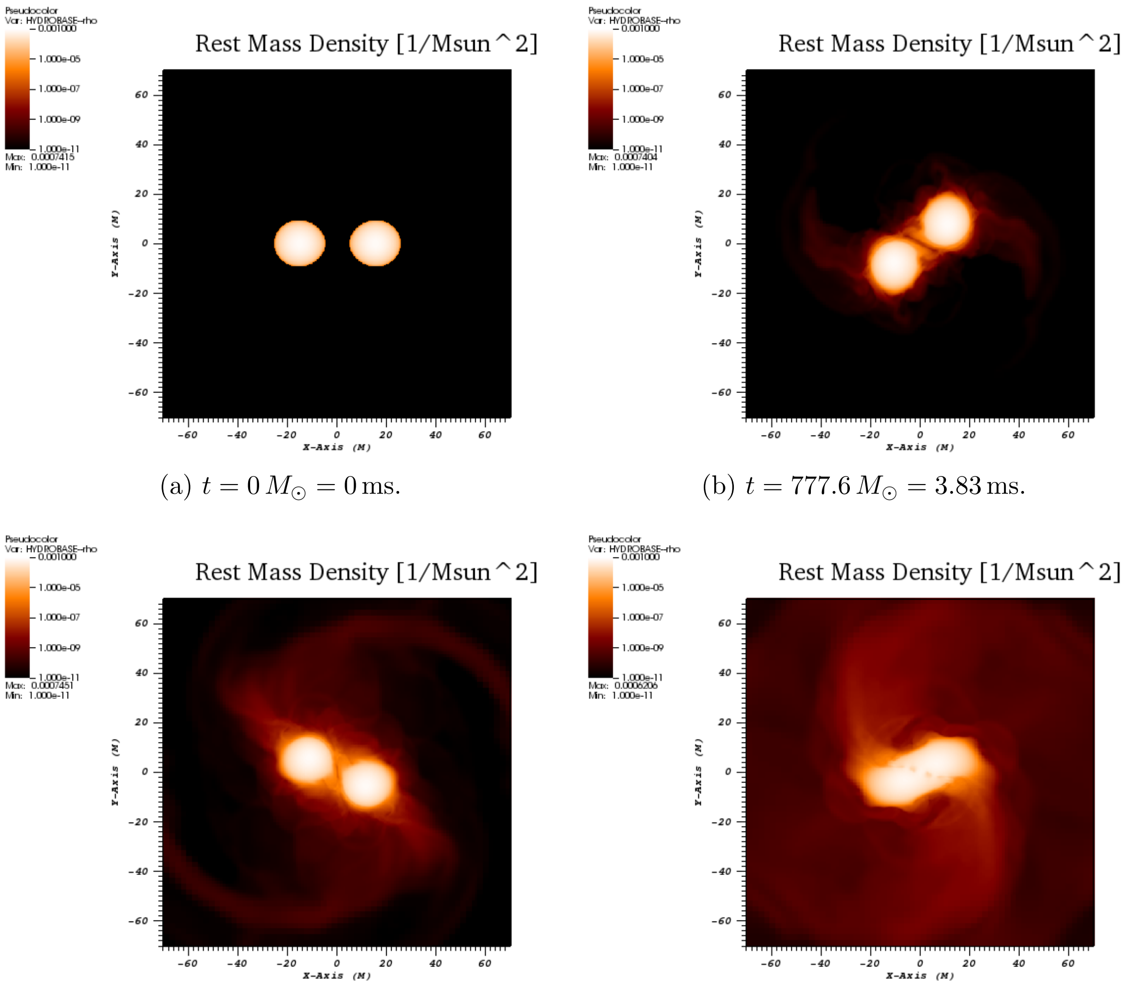

(a) $t = 0\,M_\odot = 0\,\mathrm{ms}$.

(b) $t = 777.6\,M_\odot = 3.83\,\mathrm{ms}$.

(c) $t = 1296\,M_\odot = 6.38\,\mathrm{ms}$.

(d) $t = 1857.6\,M_\odot = 9.1515\,\mathrm{ms}$.

Figure 17: .

Final stage of the rest mass density evolution

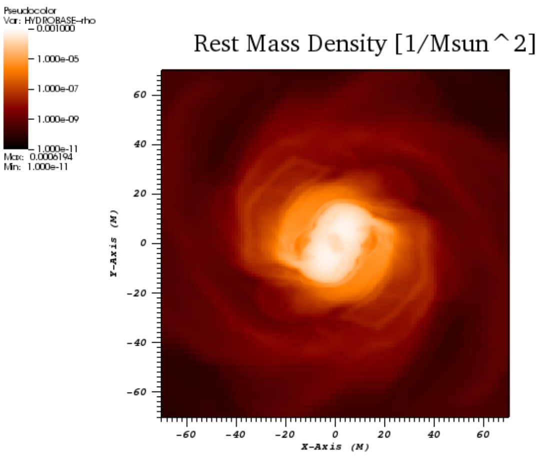

(a) $t = 2203.2\,M_\odot = 10.85\,\mathrm{ms}$.

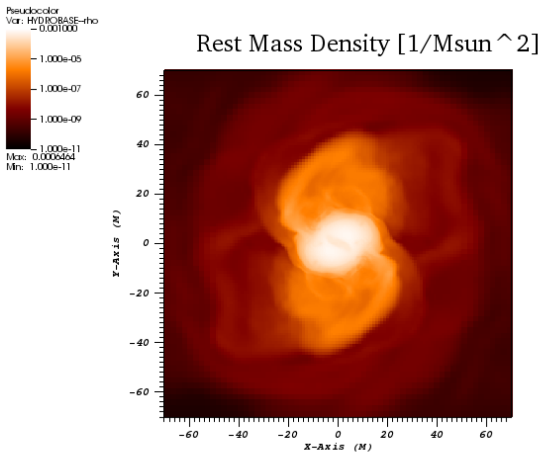

(b) $t = 2332.8\,M_\odot = 11.49\,\mathrm{ms}$.

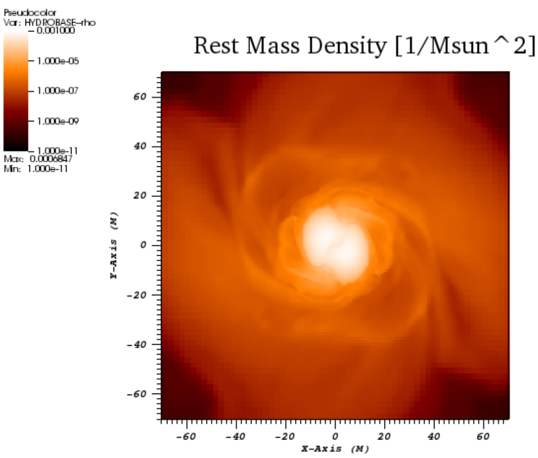

(c) $t = 2721.6\,M_\odot = 13.41\,\mathrm{ms}$.

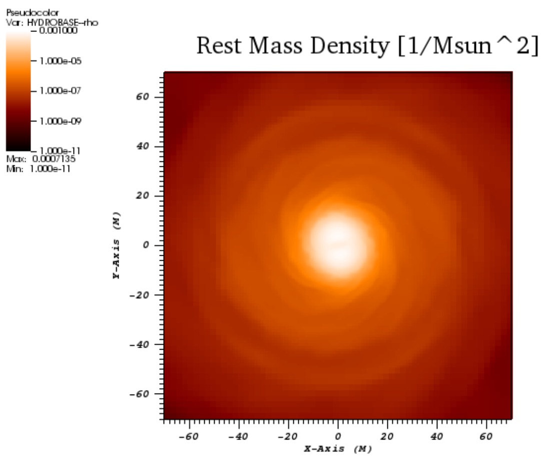

(d) $t = 3888\,M_\odot = 19.15\,\mathrm{ms}$.

Figure 18: .

6 Conclusion

7 Appendices

jajdc.,jdac amdadada [1]

References

[1] Keisuke Taniguchi and Eric Gourgoulhon. “Various Features of Quasiequilibrium Sequences of Binary Neutron Stars in General Relativity”. In: *Physical Review D* 68.12 (Dec. 2003). ISSN: 0556-2821, 1089-4918. DOI: 10.1103/PhysRevD.68.124025. arXiv: gr-qc/0309045.